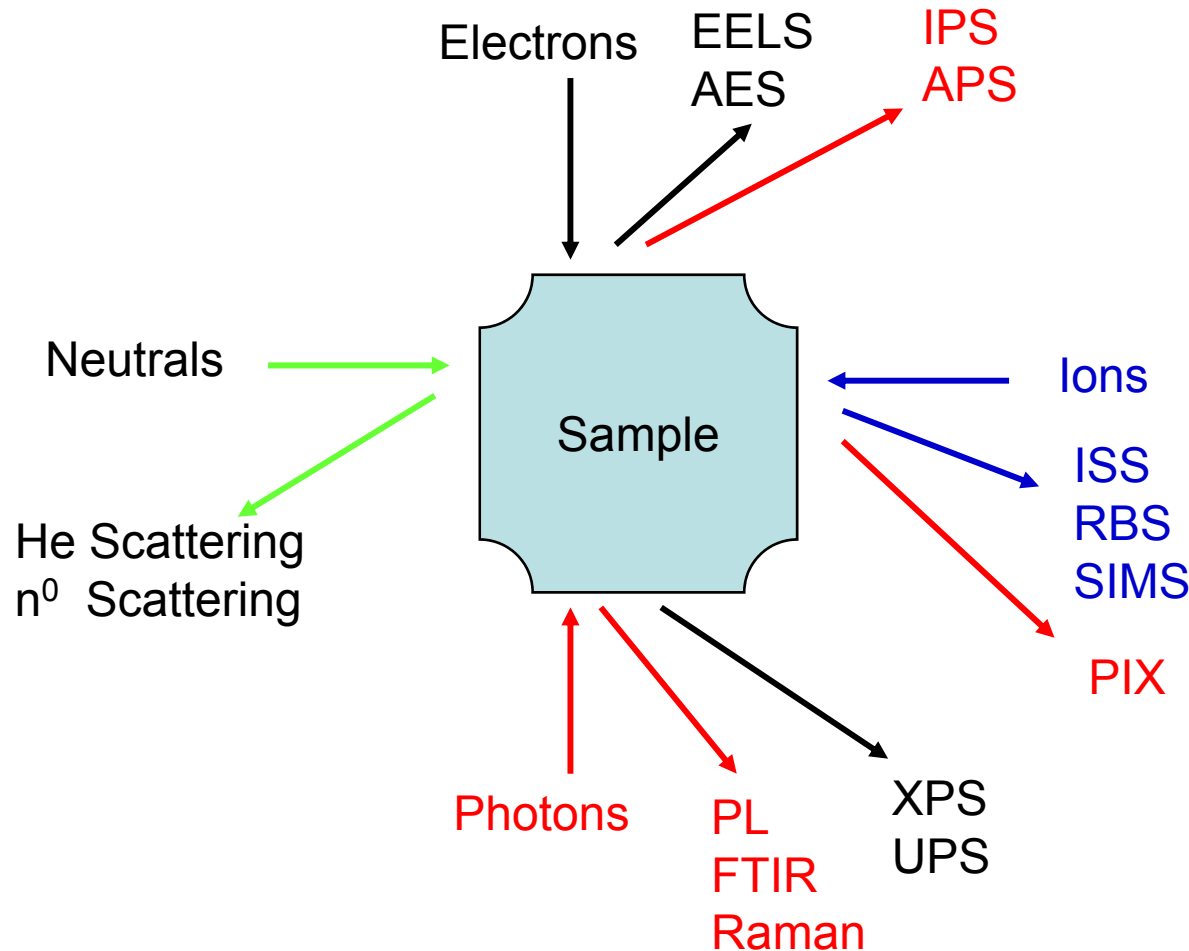


Spectroscopy at nanometer scale

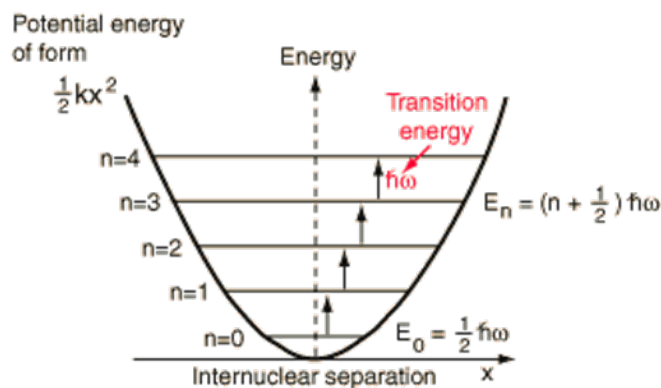
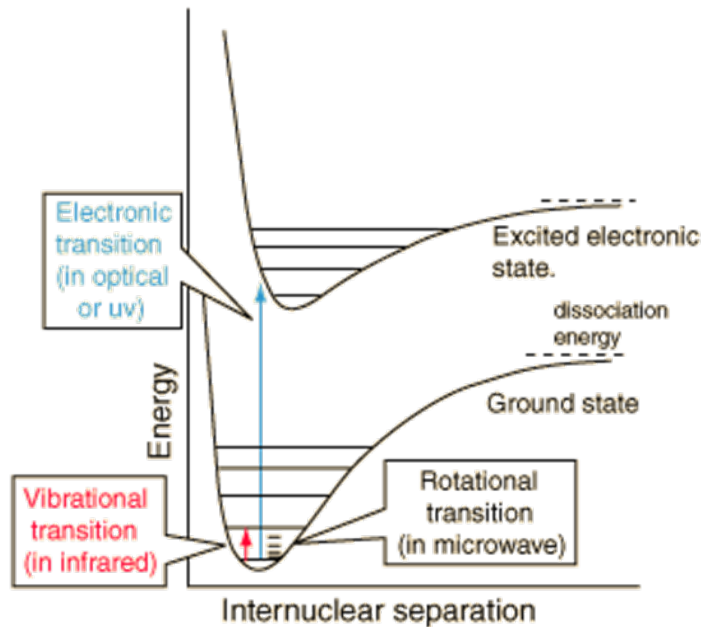
1. Physics of the spectroscopies
2. Spectroscopies for the bulk materials
3. Experimental setups for the spectroscopies
4. Physics and Chemistry of nanomaterials

Various spectroscopic methods



Born-Oppenheimer Approximation

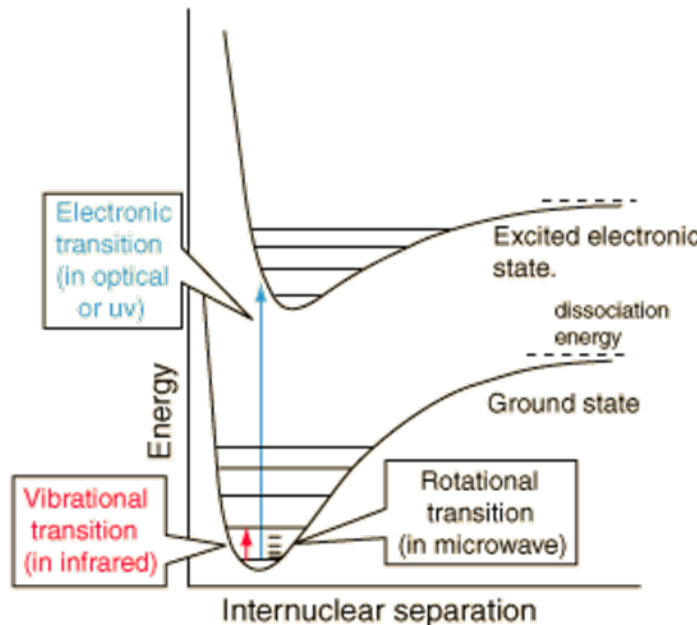
$$\Psi_{\text{molecule}}(\vec{r}_i, \vec{R}_j) = \Psi_{\text{electrons}}(\vec{r}_i, \vec{R}_j) \Psi_{\text{nuclei}}(\vec{R}_j)$$

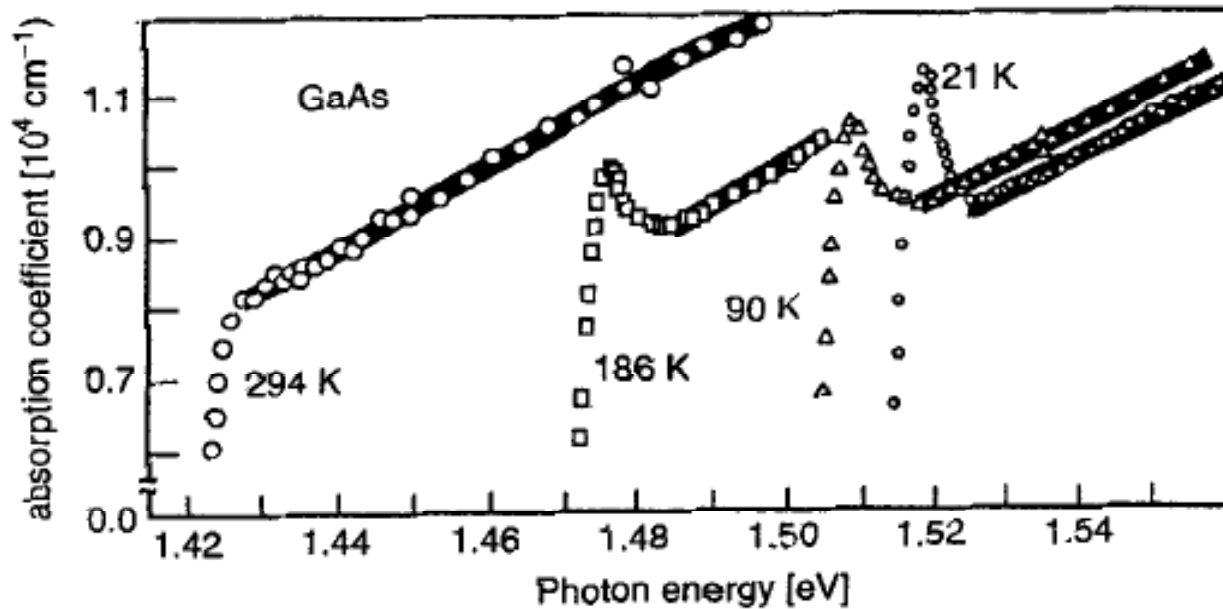


$x=0$ represents the equilibrium separation between the nuclei.

Electronic Spectroscopy

1. Photons in, photons out – PL
2. Photons in, electrons out – UPS, XPS
3. Electrons in, electrons out – EELS





Binding energy and effective radius for the exciton

$$E_e = (m^*/m_e)(\epsilon/\epsilon_0)^{-2} \text{ (13.6 eV)}$$

$$a_{\text{eff}} = (\epsilon/\epsilon_0)(m^*/m_e)^{-1} \text{ (0.0529 nm)}$$

For GaAs, $\epsilon/\epsilon_0 \sim 13.2$ and $m^* \sim 0.067 m_e$

then $E_e \sim 5 \text{ meV}$ and $a_{\text{eff}} \sim 10 \text{ nm}$

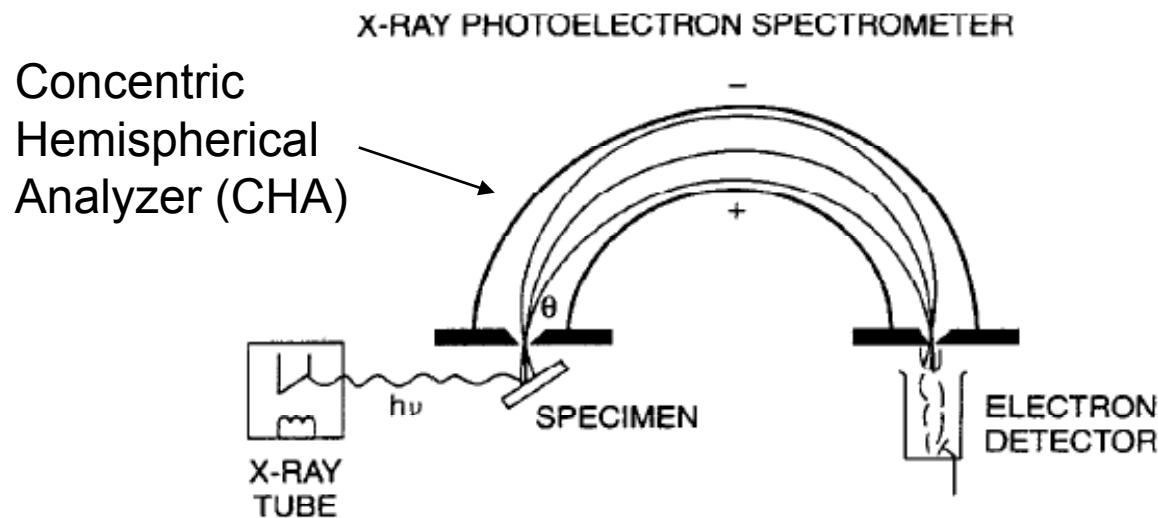
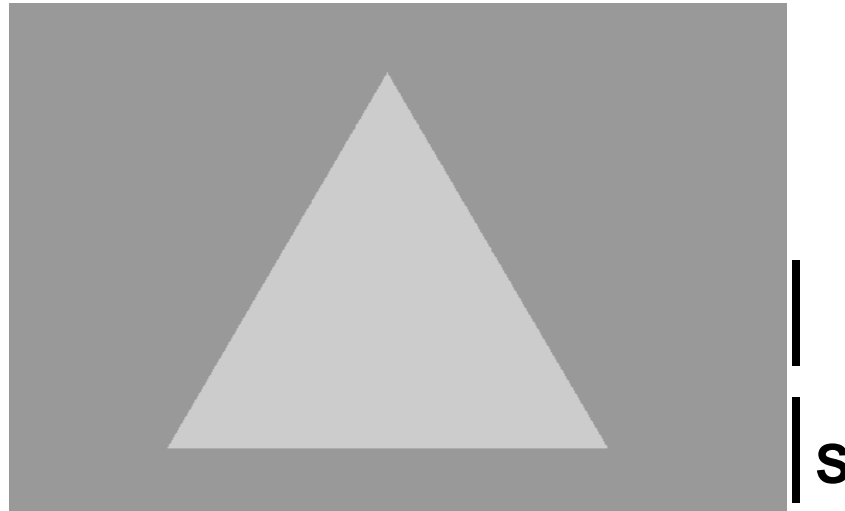
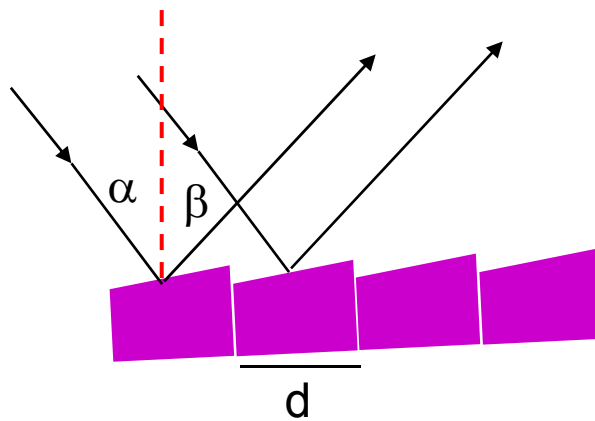


Figure 3.29. X-ray photoelectron spectrometer showing photons $h\nu$ generated by an X-ray tube incident on the specimen where they produce photoelectrons e^- characteristic of the specimen material, which then traverse a velocity analyzer, and are brought to focus at an electron detector that measures their kinetic energy.

Prism



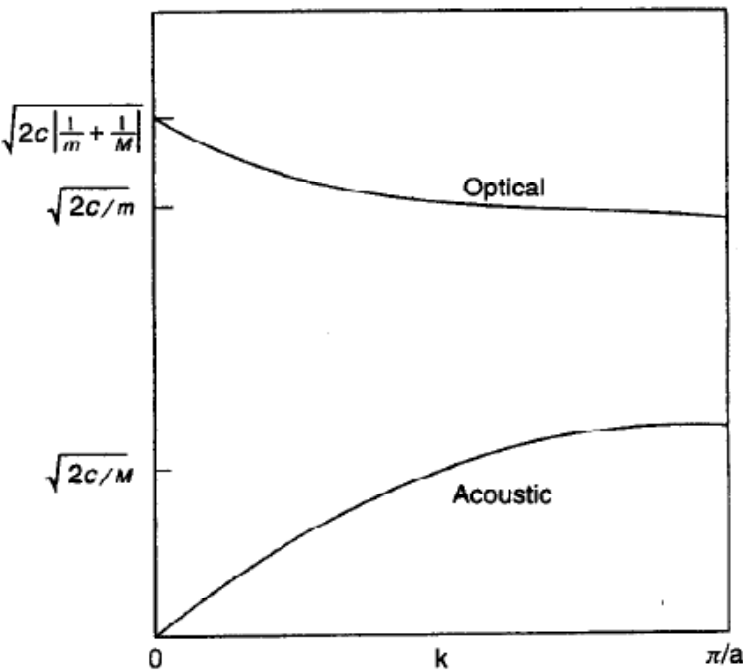
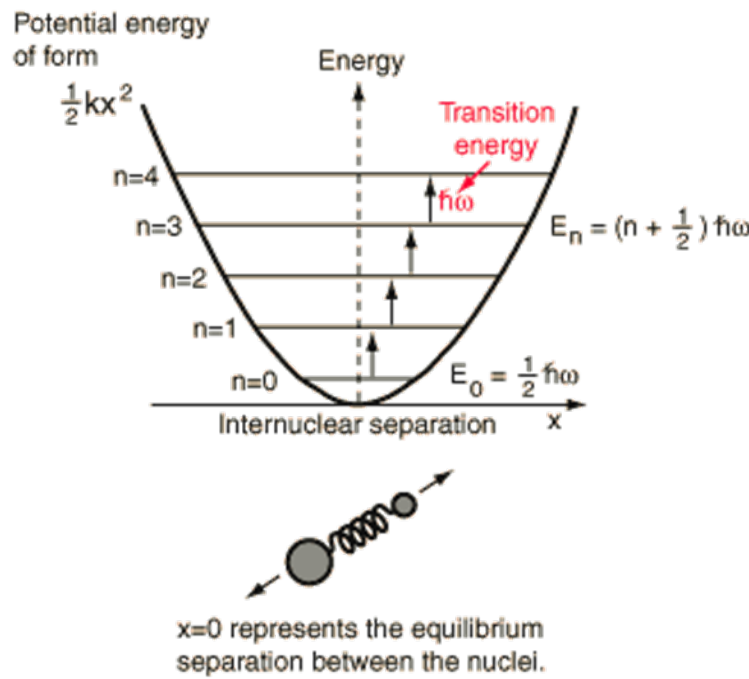
Grating



$$\Delta s = d (\sin \alpha - \sin \beta) = m\lambda$$

Vibrational Spectroscopy

1. Photons in, photons out – IR, Raman
2. Electrons in, electrons out – EELS



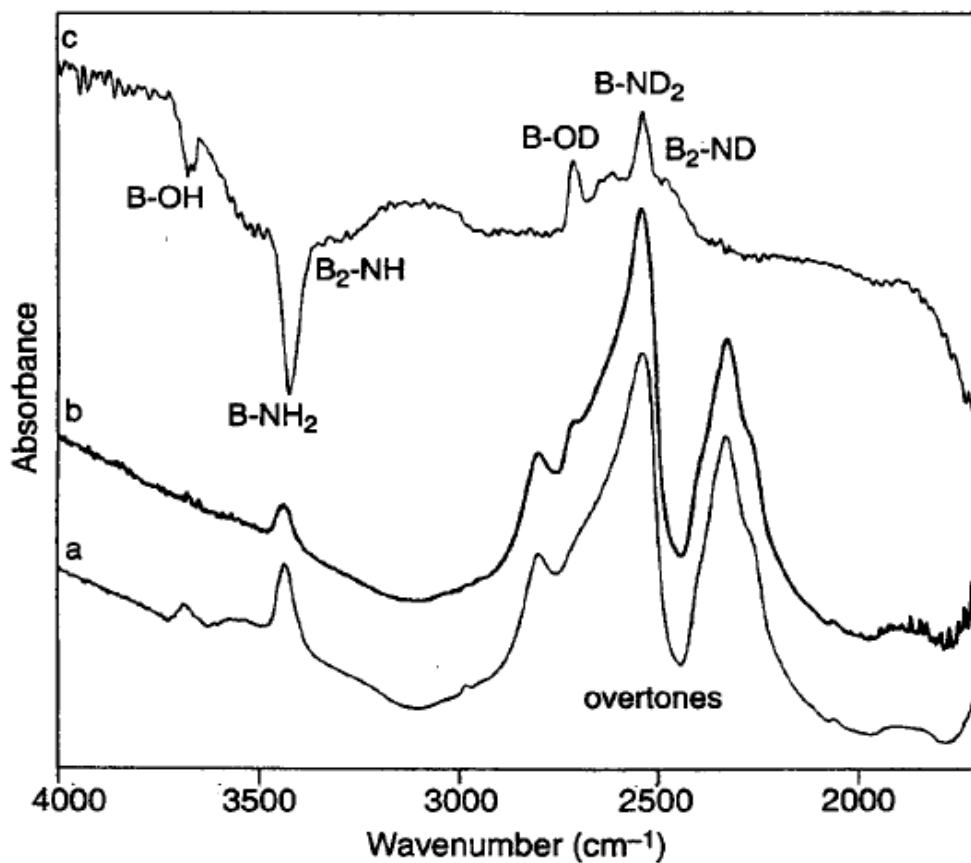


Figure 8.5. FTIR spectra of boron nitride nanopowder surfaces after activation at 875 K (tracing a), after subsequent deuteration (tracing b), and (c) difference spectrum of a subtracted from b (tracing c). [From M.-I. Baraton and L. Merhari, P. Quintard, V. Lorezenvilli, *Langmuir*, 9, 1486 (1993).]

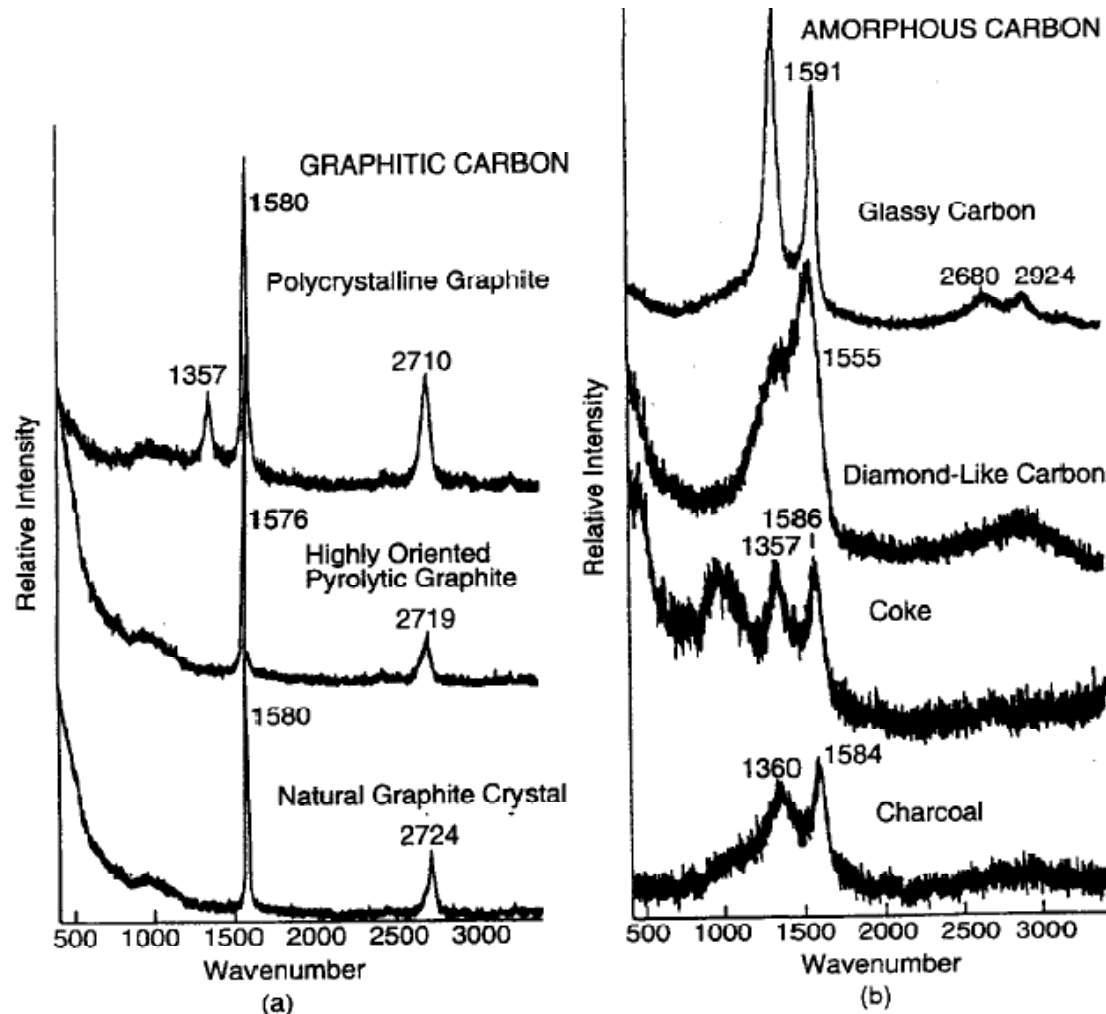
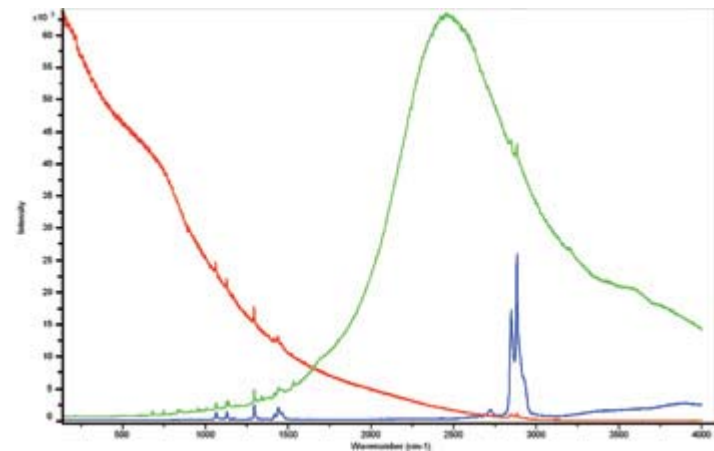
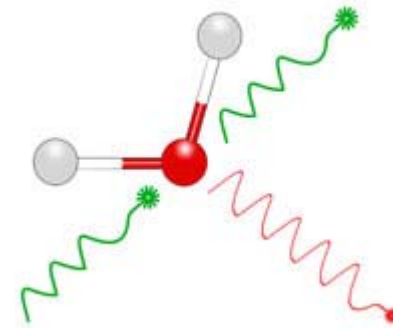
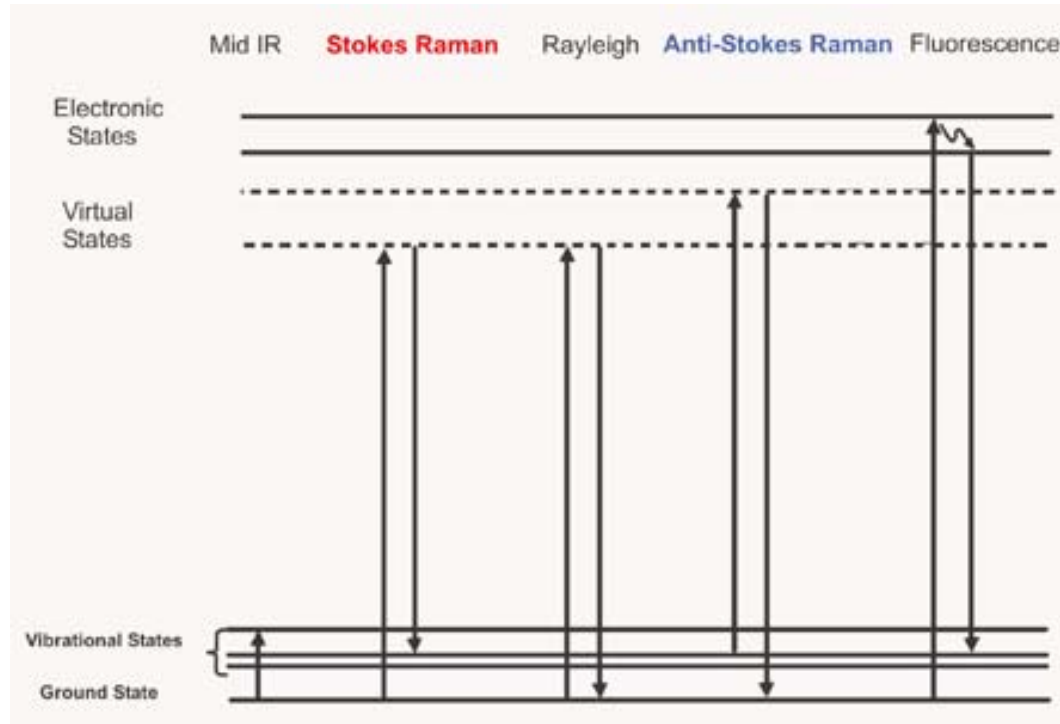
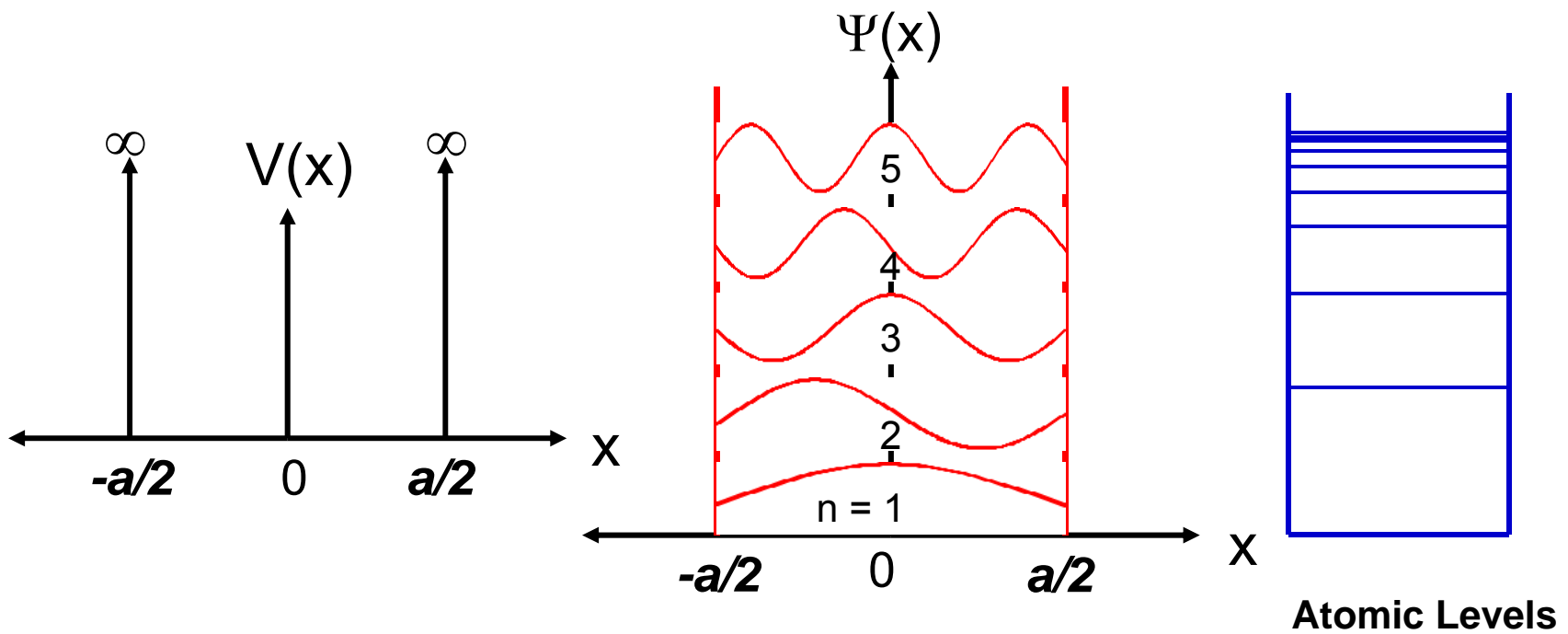


Figure 8.19. Raman spectra of (a) crystalline graphites and (b) noncrystalline, mainly graphitic, carbons. The *D* band appears near 1355cm^{-1} and the *G* band, near 1580cm^{-1} . [From D. S. Knight and W. B. White, *J. Mater. Sci.* **4**, 385 (1989).]

The Theory of Raman Spectroscopy



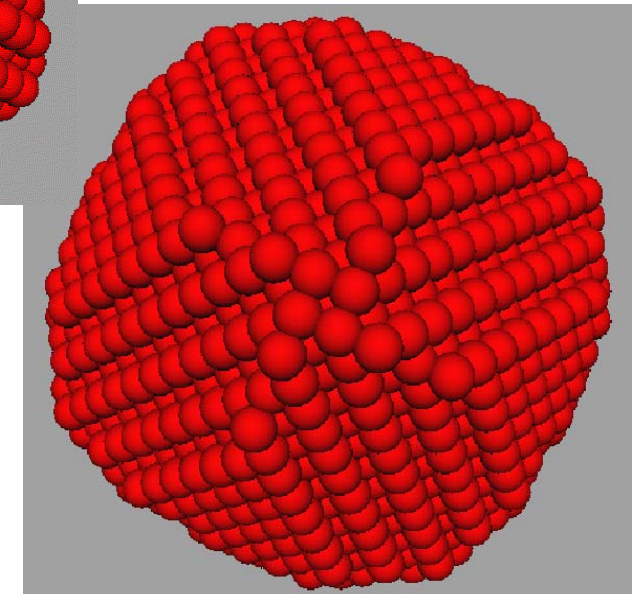
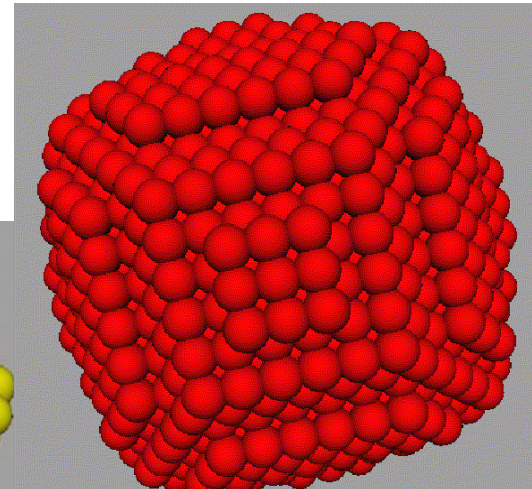
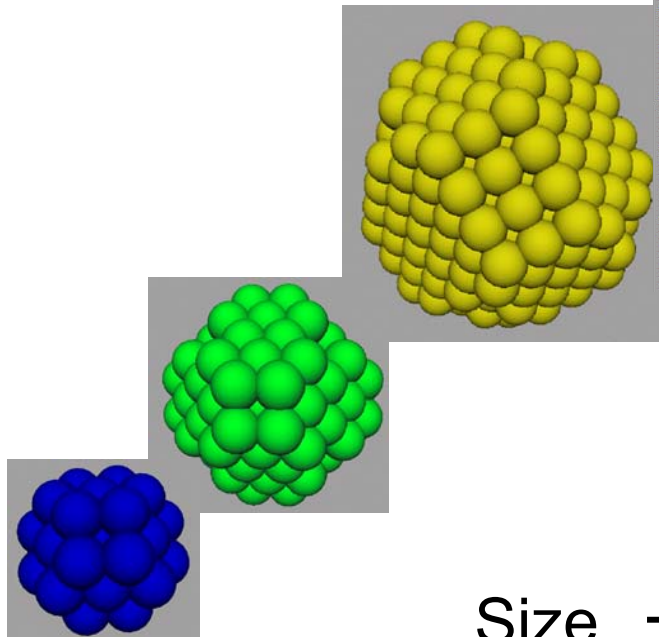
One dimensional size effect



$$\Psi(x) = \begin{cases} \sin(n\pi x/a), & n \text{ even} \\ \cos(n\pi x/a), & n \text{ odd} \end{cases}$$

$$E = n^2\pi^2\hbar^2/2ma^2, \quad n = 1, 2, 3, \dots$$

Size effect



CHANGE IN VALENCE ENERGY BAND LEVELS WITH SIZE



BULK METAL

(a)



LARGE METAL CLUSTER

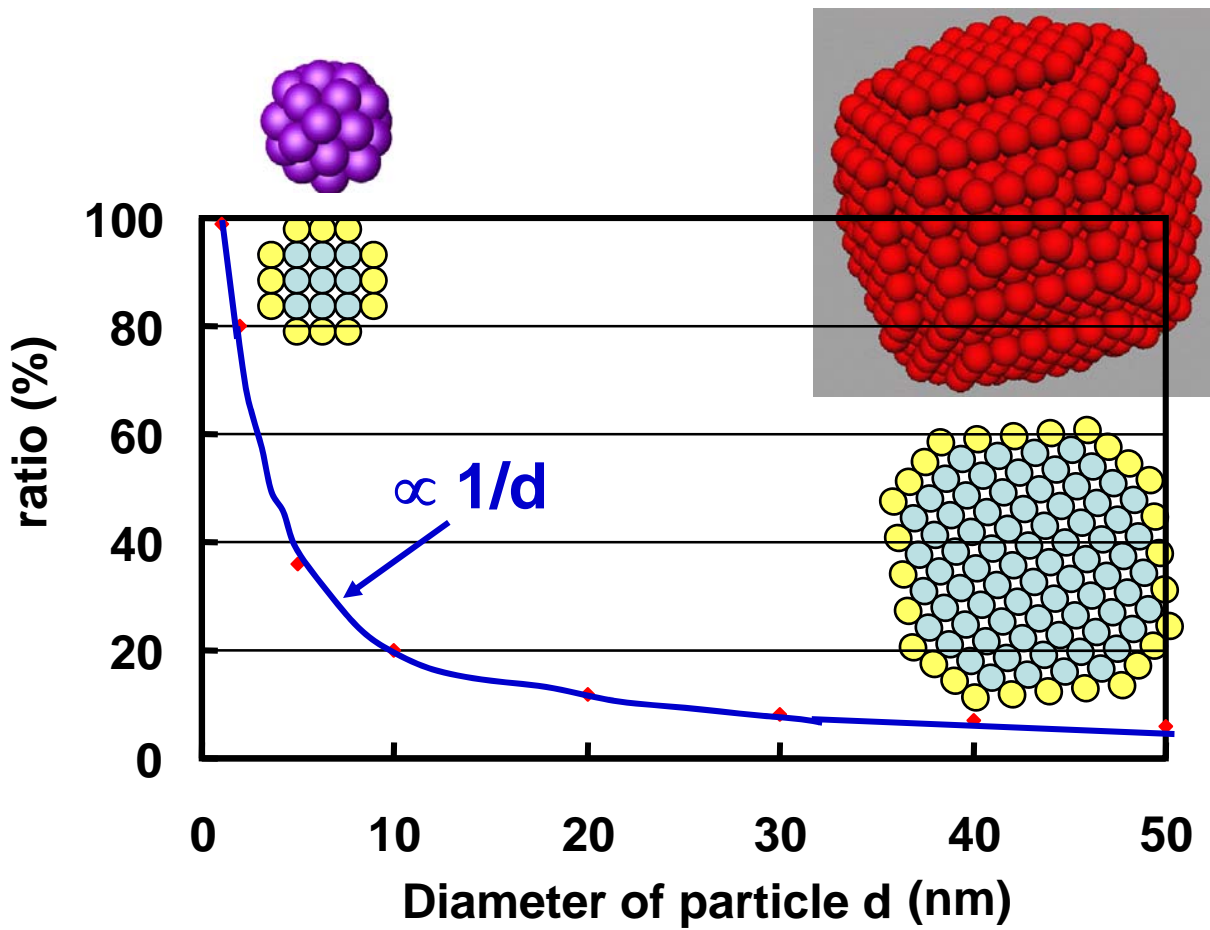
(b)



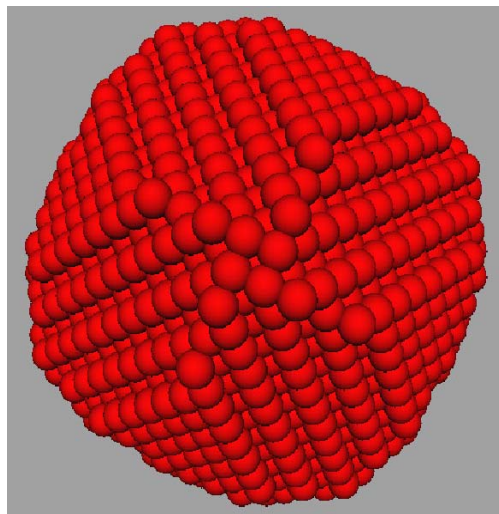
SMALL METAL CLUSTER

(c)

Ratio of surface atoms



Au nanoparticle as an example



← 10 nm →

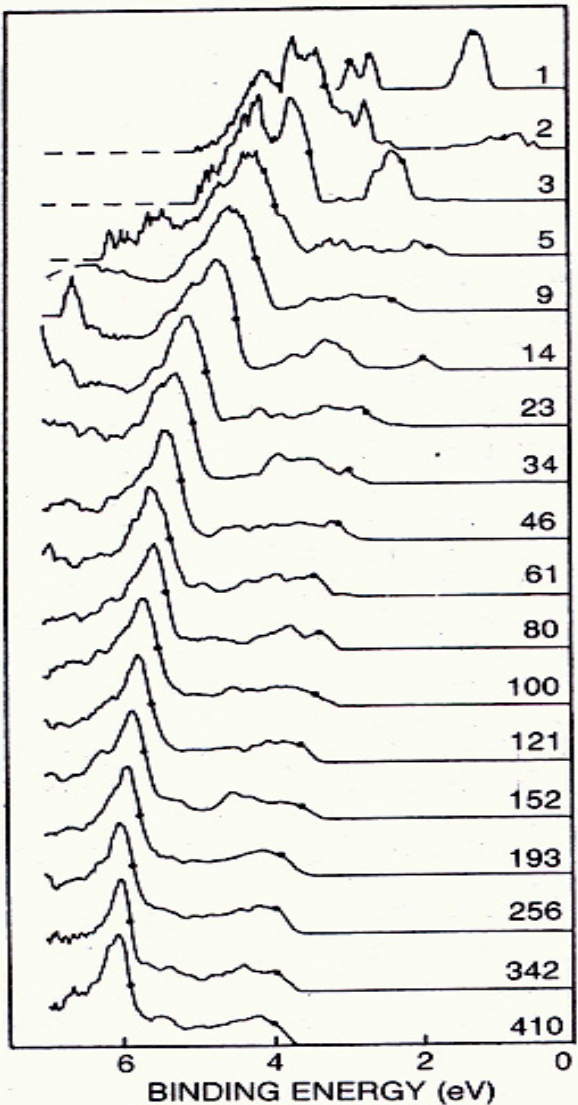
$$E_F = (\hbar^2/2m) (3\pi^2n)^{2/3}$$

$$g(E_F) = (3/2) (n/E_F)$$

$$\delta = 2/[g(E_F)V] = (4/3) (E_F/N)$$

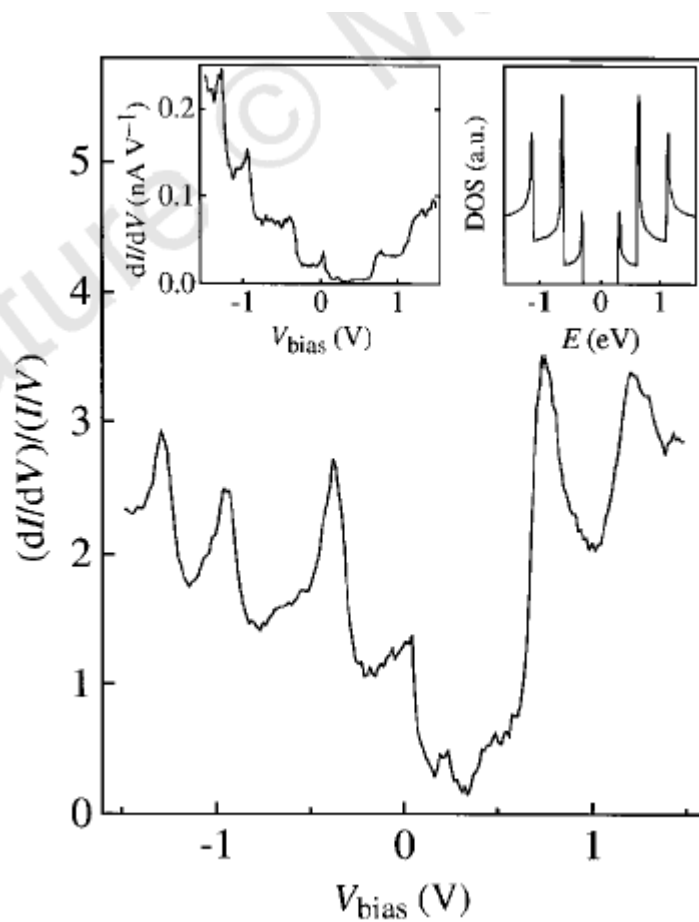
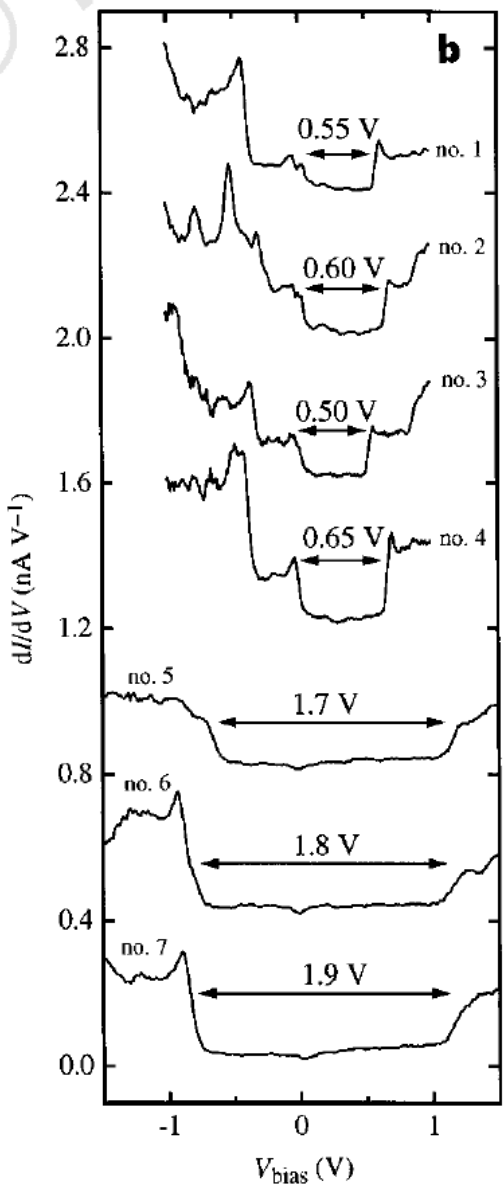
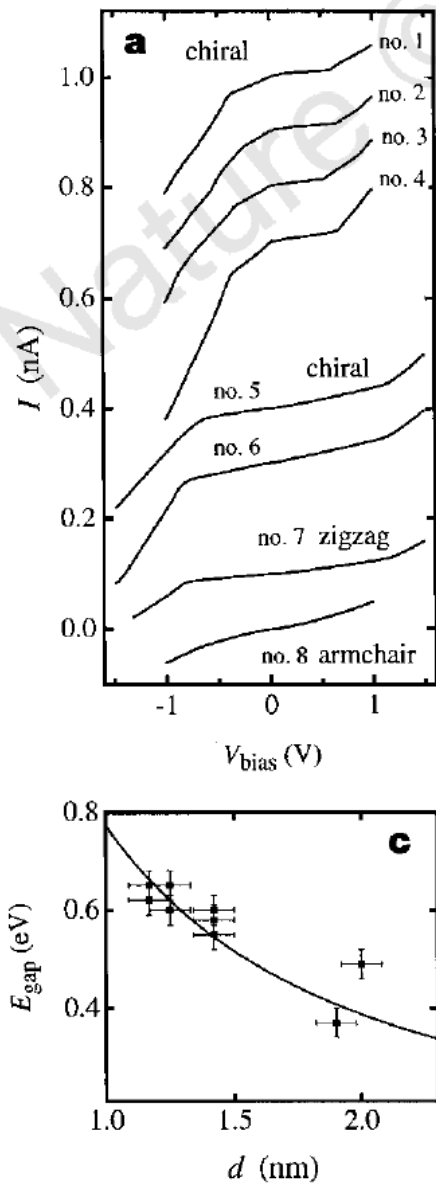
Number of valence electrons (N) contained in the particles is roughly 40,000. Assume the Fermi energy (E_F) is about 7 eV for Au, then

$$\delta \sim 0.22 \text{ meV} \sim 2.5 \text{ K}$$



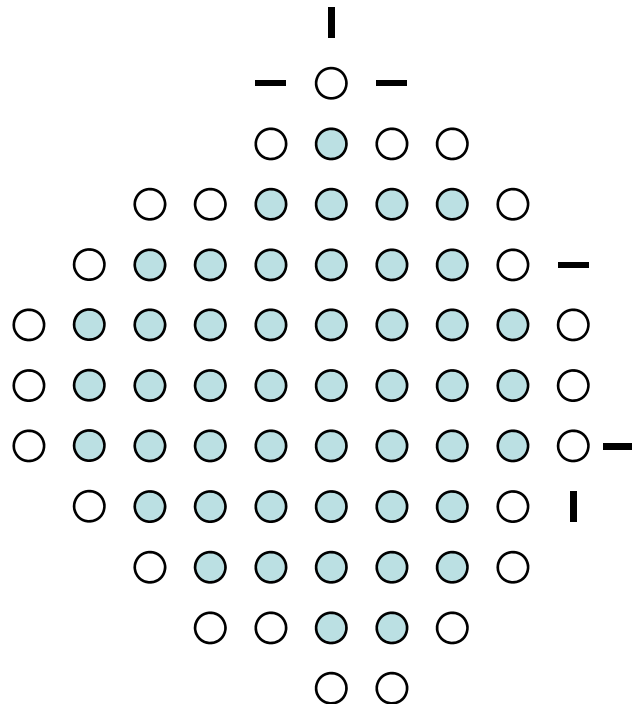
Ultraviolet photoemission spectra of ionized copper clusters Cu_N^- ranging in size from N of 1 to 410 show the energy distribution versus binding energy of photoemitted electrons. These photoemission patterns show the evolution of the 3d band of Cu as a function of cluster size. As the cluster size increases, the electron affinity approaches the value of the bulk metal work function. (Adapted from ref. 10.) **Figure 5**

Electronic Structure of Single-wall Nanotubes



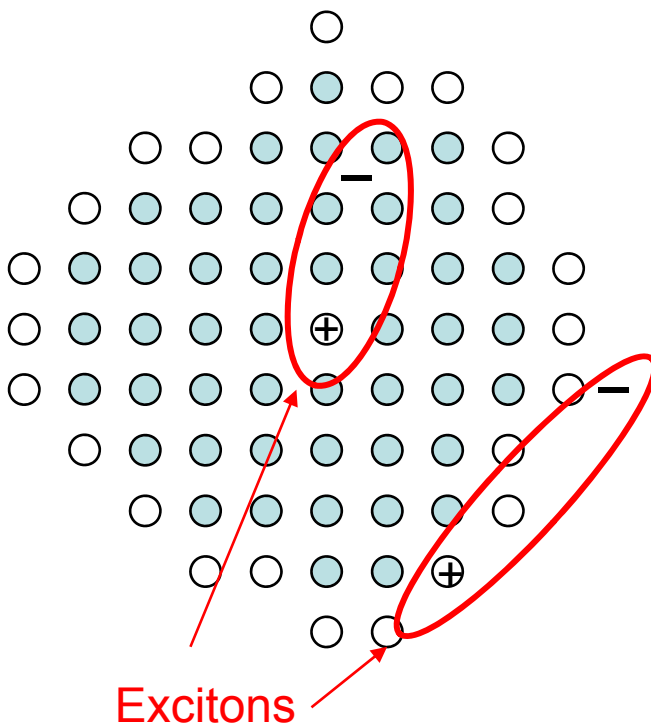
Nature 391, 59 (1998).

Optical properties of nanoparticles (in the infrared range)



- (1) Broad-band absorption:
Due mainly to the increased normal modes at the surface.
- (2) Blue shift:
Due mainly to the bond shortening resulted from surface tension.

Optical properties of nanoparticles (in the visible light range)



(1) Blue shift:

Due mainly to the energy-gap widening because of the size effect.

(2) Red shift:

Bond shortening resulted from surface tension causes more overlap between neighboring electron wavefunctions. Valence bands will be broadened and the gap becomes narrower.

(3) Enhanced exciton absorption:

Due mainly to the increased probability of exciton formation because of the confining effect.

Optical properties

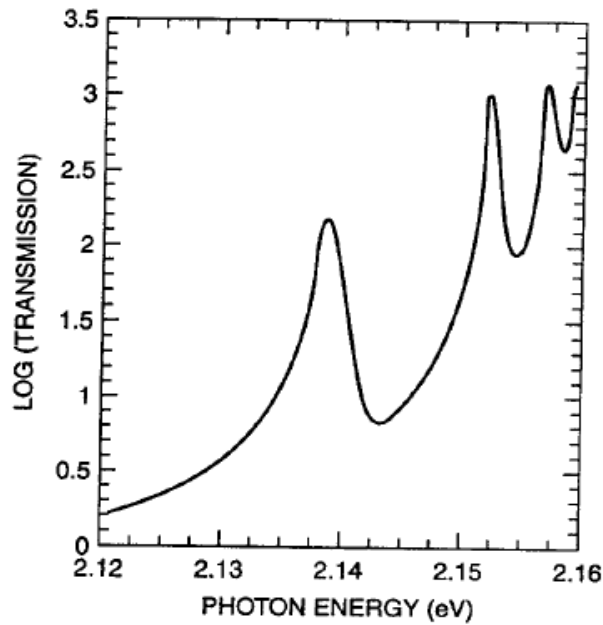


Figure 4.19. Optical absorption spectrum of hydrogen-like transitions of excitons in Cu₂O.
[Adapted from P. W. Baumeister, *Phys. Rev.* **121**, 359 (1961).]

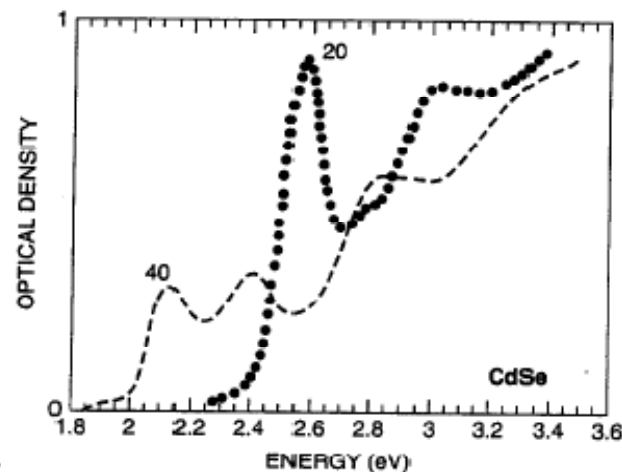
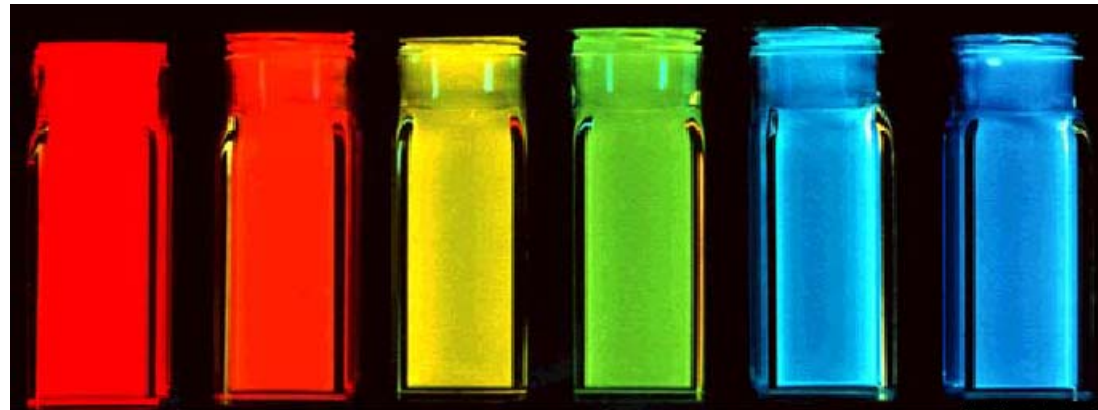
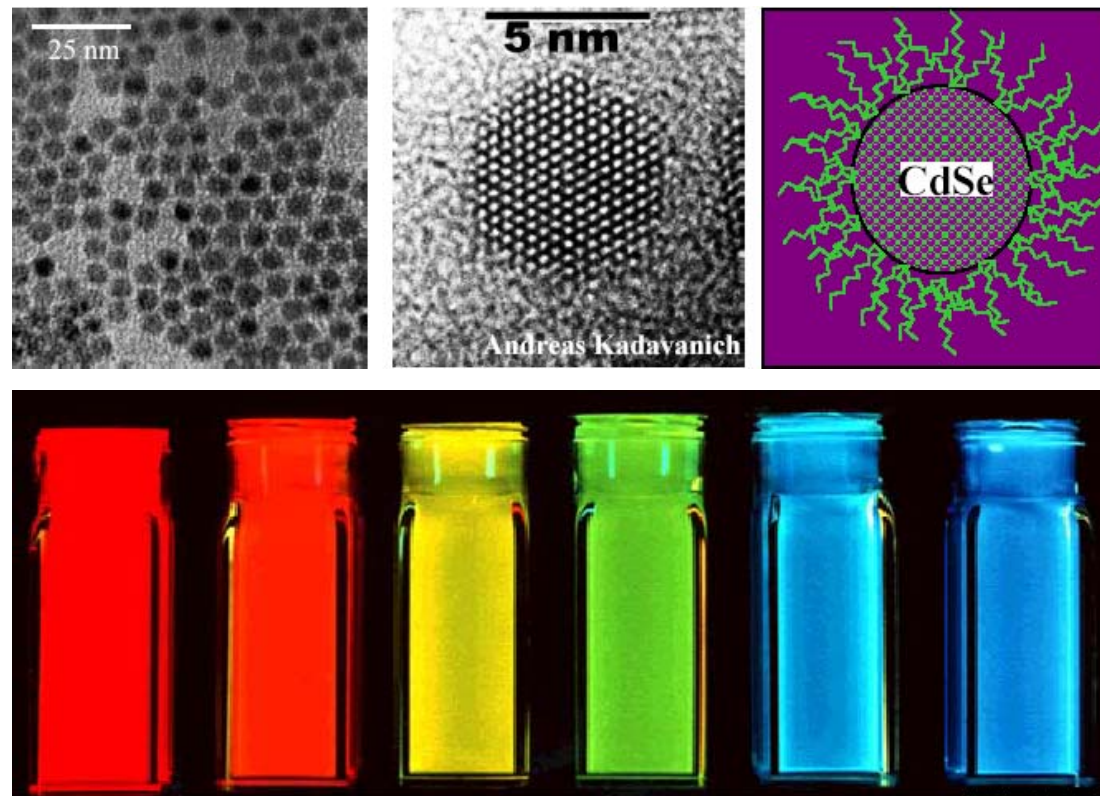
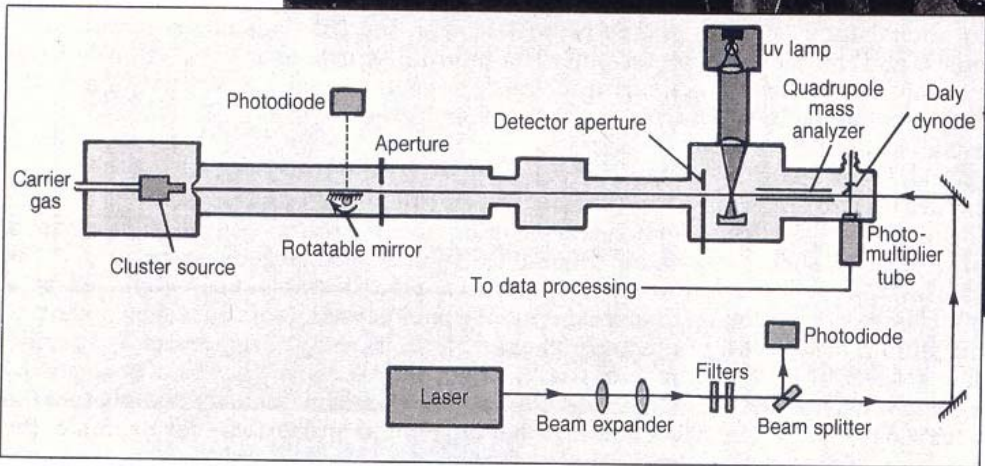
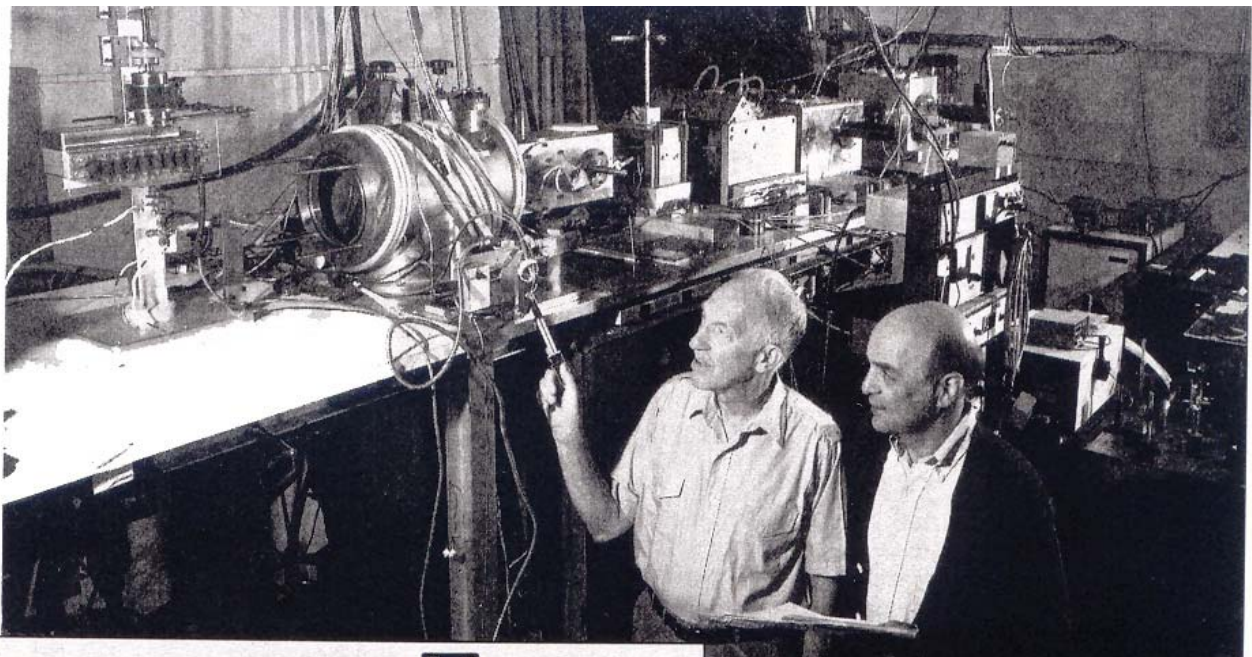


Figure 4.20. Optical absorption spectrum of CdSe for two nanoparticles having sizes 20 Å and 40 Å, respectively. [Adapted from D. M. Mittleman, *Phys. Rev.* **B49**, 14435 (1994).]

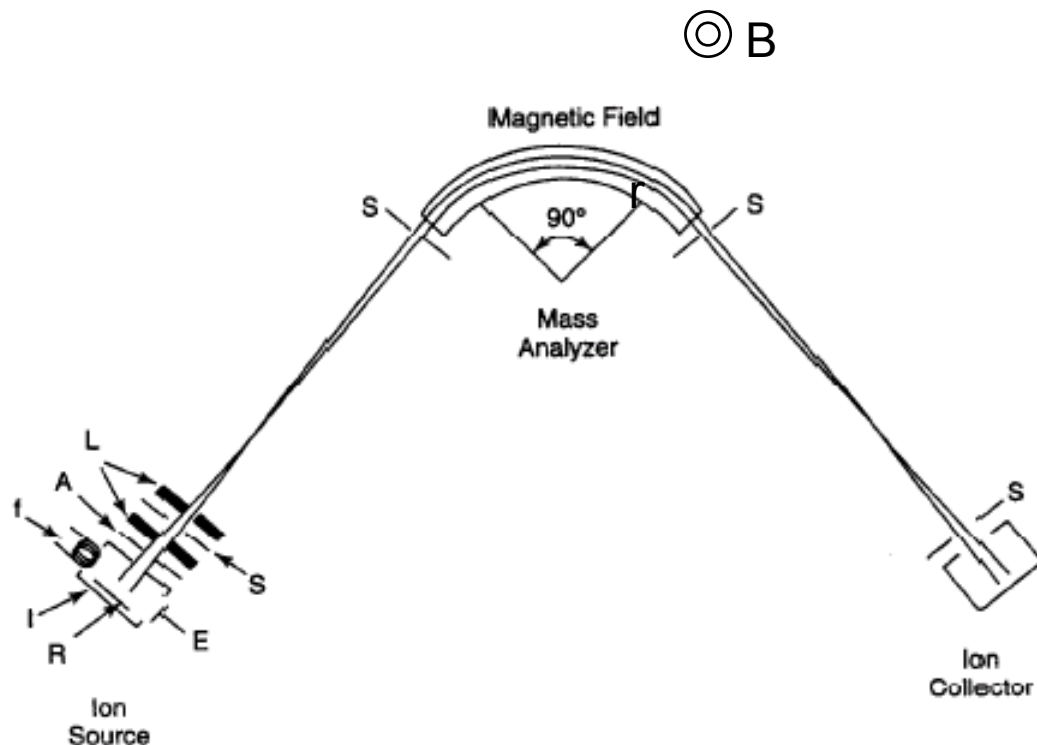
Semiconductor quantum dots



(Reproduced from Quantum Dot Co.)



Mass Analyzer



◎ B

$$qV = \frac{1}{2} mv^2$$

$$F = qvB = mv^2/r$$

$$m/q = \frac{1}{2} B^2 r^2/V$$

Figure 3.8. Sketch of a mass spectrometer utilizing a 90° magnetic field mass analyzer, showing details of the ion source: A—accelerator or extractor plate, E—electron trap, f—filament, I—ionization chamber, L—focusing lenses, R—repeller, S—slits. The magnetic field of the mass analyzer is perpendicular to the plane of the page.

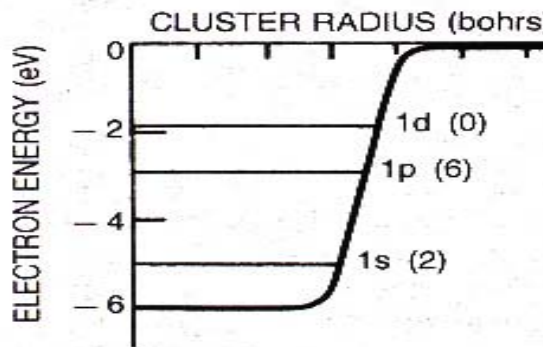
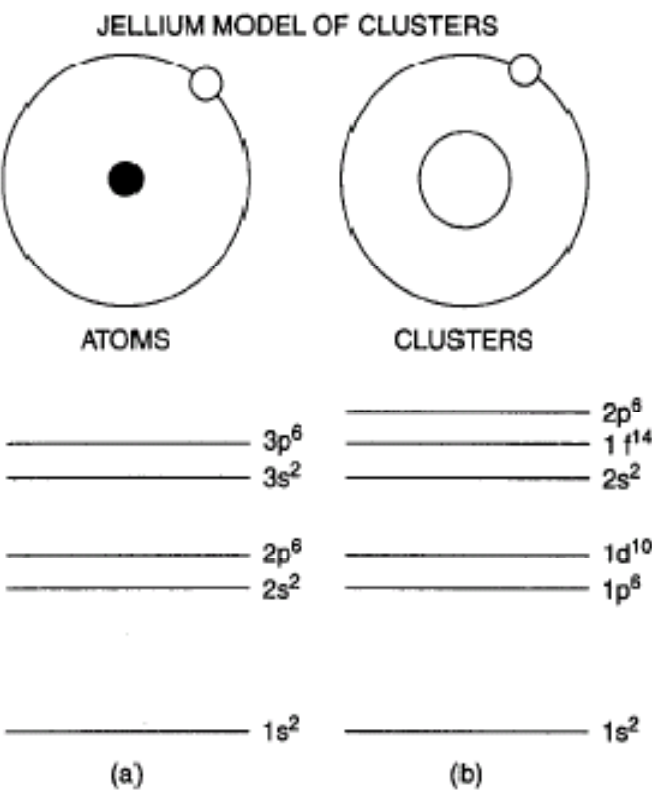
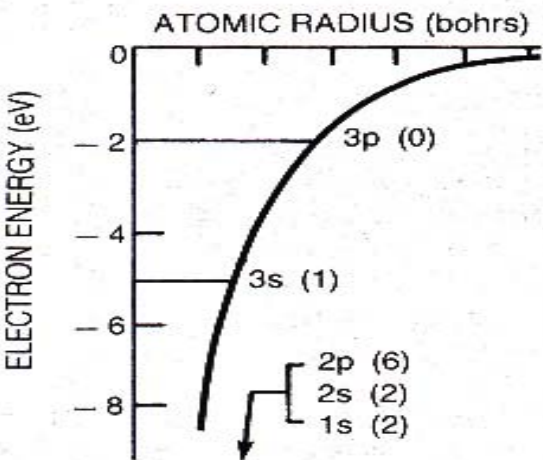
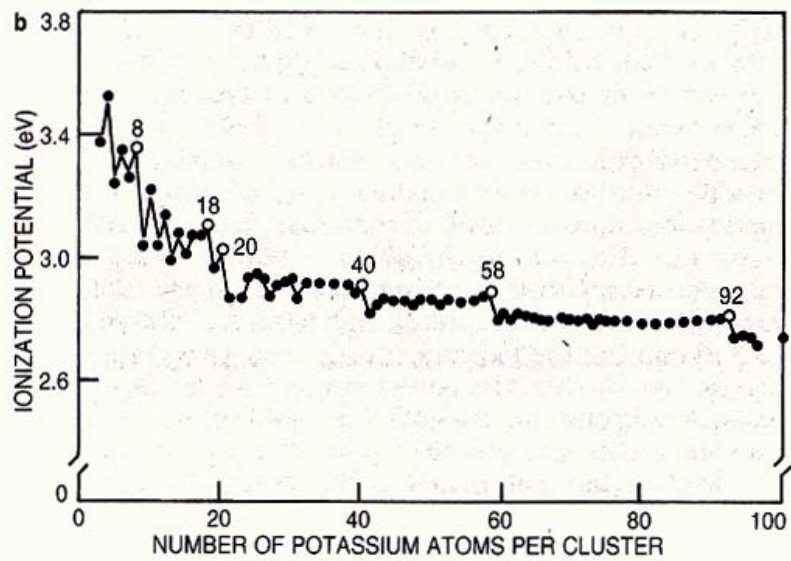
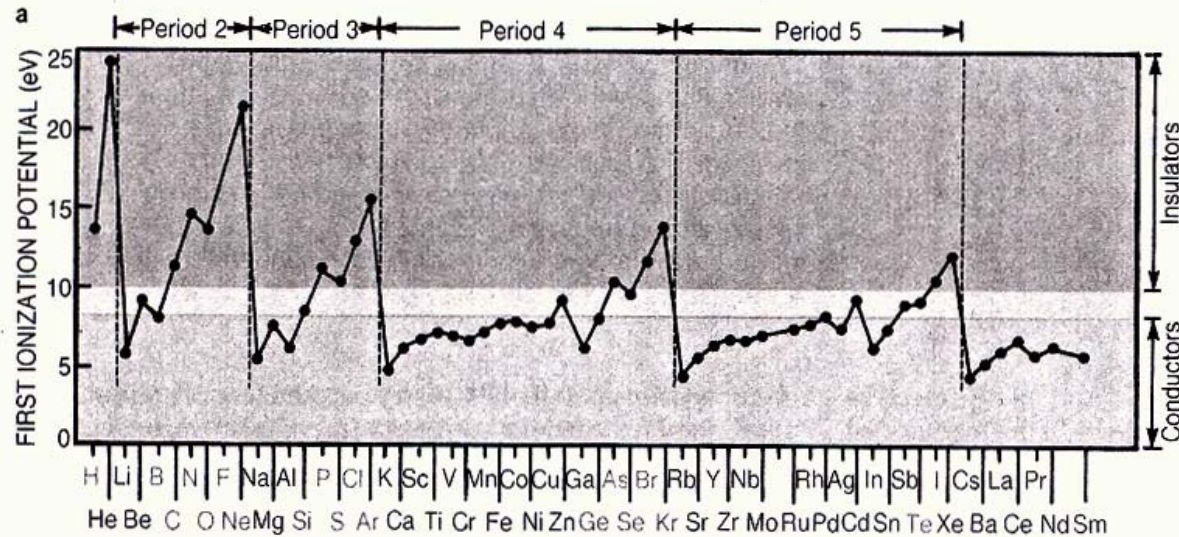
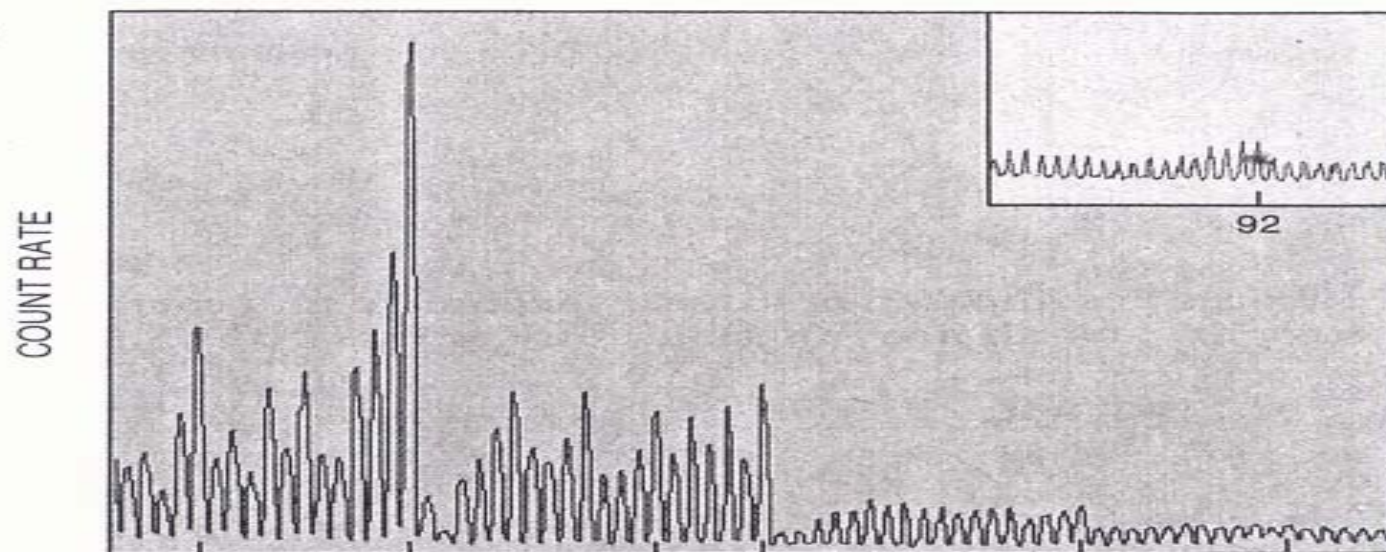
a**c****b**

Figure 4.5. A comparison of the energy levels of the hydrogen atom and those of the jellium model of a cluster. The electronic magic numbers of the atoms are 2, 10, 18, and 36 for He, Ne, Ar, and Kr, respectively (the Kr energy levels are not shown on the figure) and 2, 18, and 40 for the clusters. [Adapted from B. K. Rao et al., *J. Cluster Sci.* **10**, 477 (1999).]

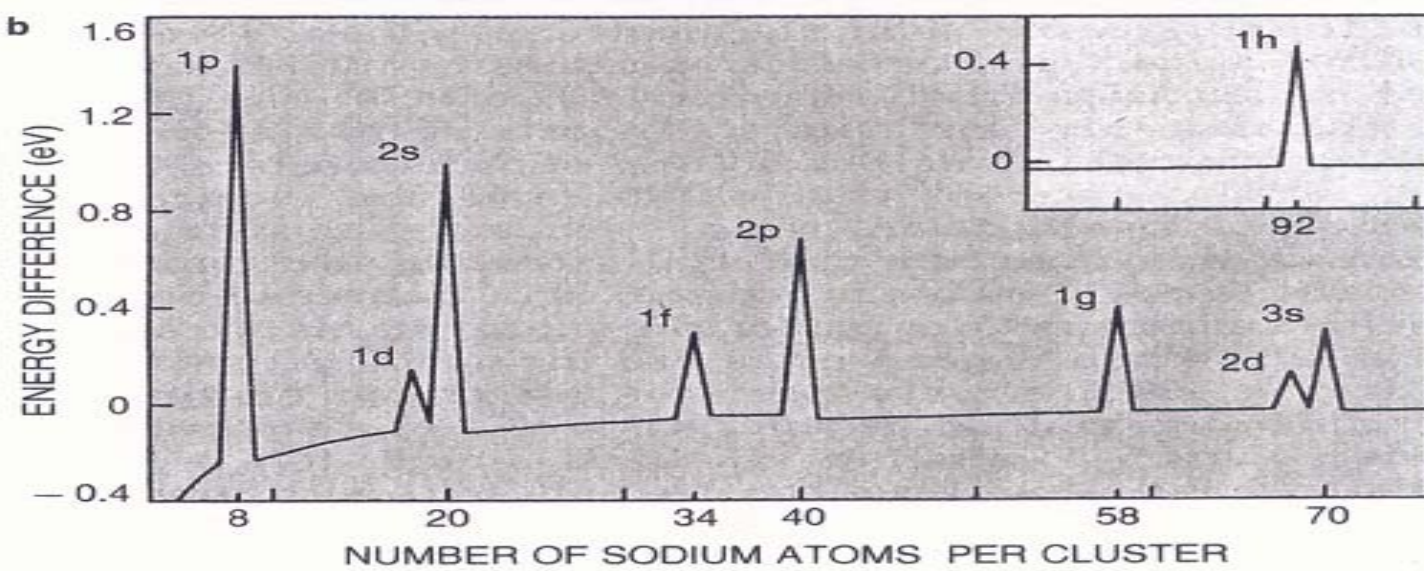


Shell structure: Two views. **a:** Atomic ionization potentials drop abruptly from above 10 eV following the shell closings for the noble gases (He, Ne, Ar and so on). For semiconductors (labeled in blue) the ionization potential is between 8 and 10 eV, while for conductors (red) it is less than 8 eV. It is clear that bulk properties follow from the natures of the corresponding atoms. (Adapted from A. Holden, *The Nature of Solids*, © Columbia U. P., New York, 1965. Reprinted by permission.) **b:** Ionization potentials for clusters of 3 to 100 potassium atoms show behavior analogous to that seen for atoms. The cluster ionization potential drops abruptly following spherical shell closings at $N = 8, 20, 40 \dots$. Features at $N = 26$ and 30 represent spheroidal subshell closings. The work function for bulk potassium metal is 2.4 eV. **Figure 3**

a



b



Reactivity of nanoclusters

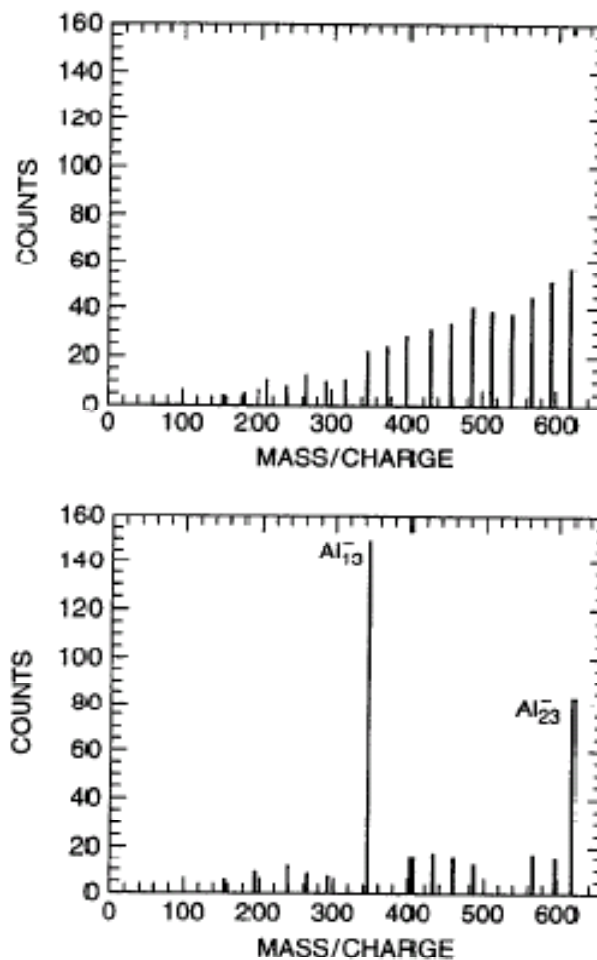


Figure 4.13. Mass spectrum of Al nanoparticles before (top) and after (bottom) exposure to oxygen gas. [Adapted from R. E. Leuchtner et al., *J. Chem. Phys.*, **91**, 2753 (1989).]

Magic clusters

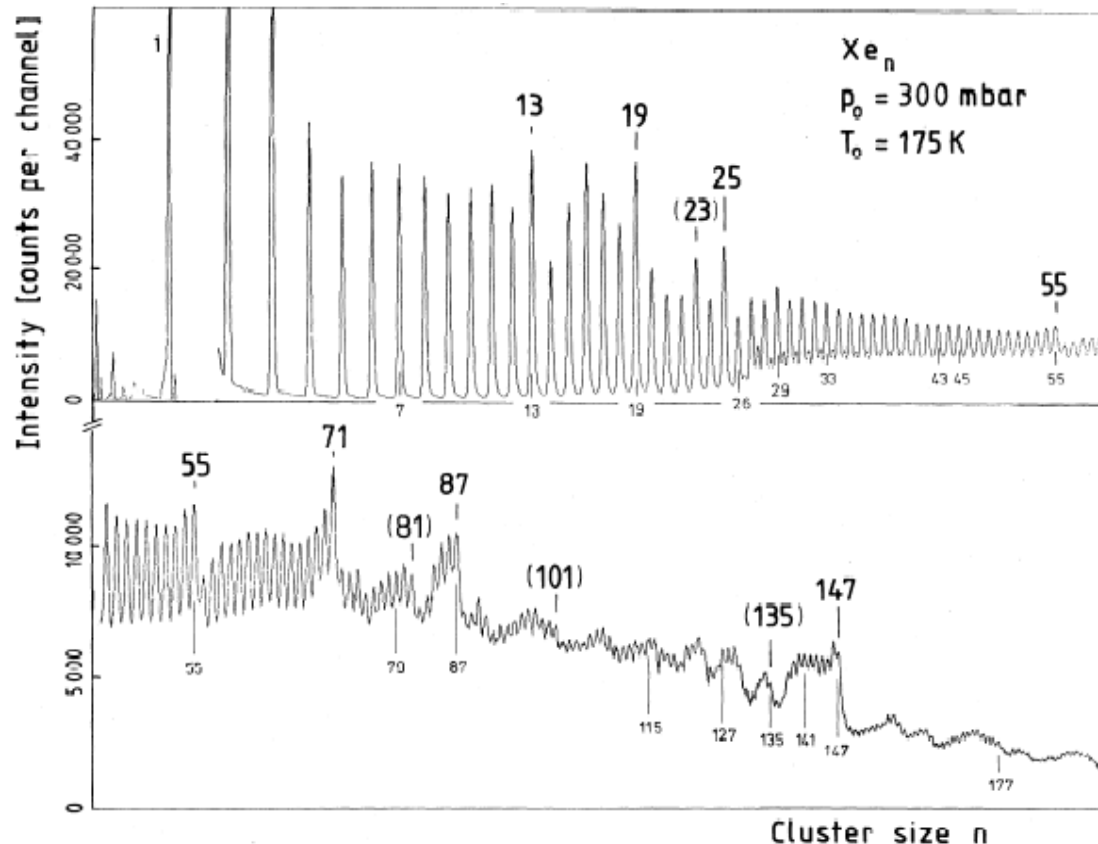
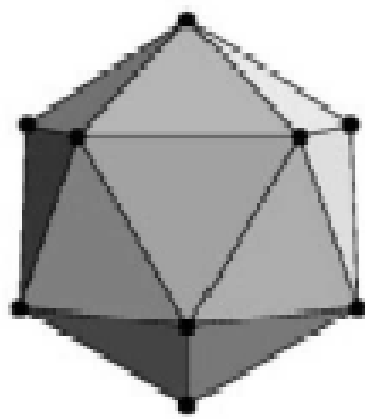


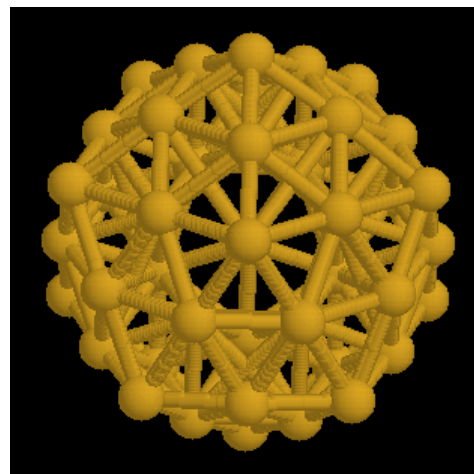
FIG. 1. Mass spectrum of xenon clusters. Observed magic numbers are marked in boldface; brackets are used for numbers with less pronounced effects. Numbers below the curve indicate predictions or distinguished sphere packings.

Mackay icosahedra

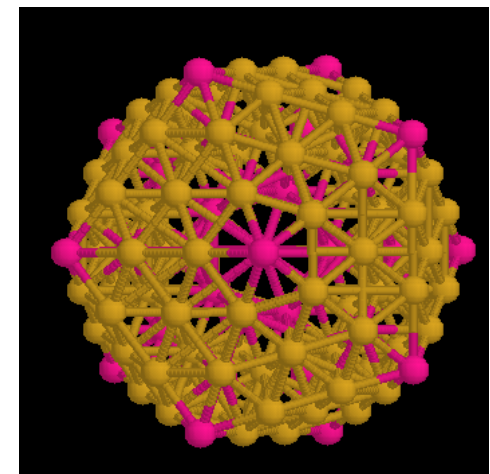


$P = 1$

20 fcc(111) faces



$P = 2$

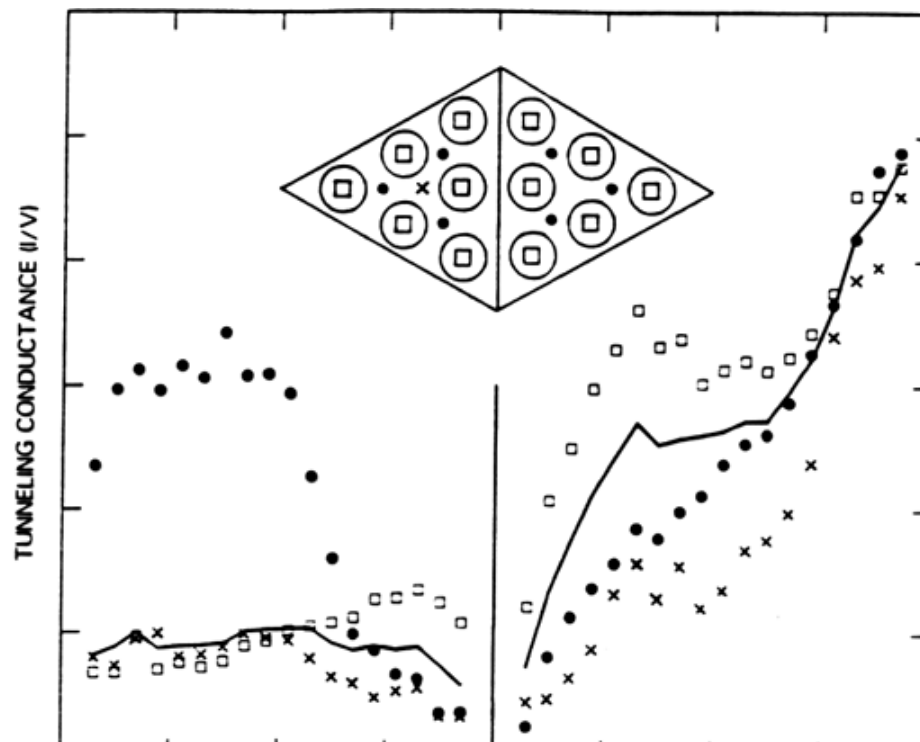


$P = 3$

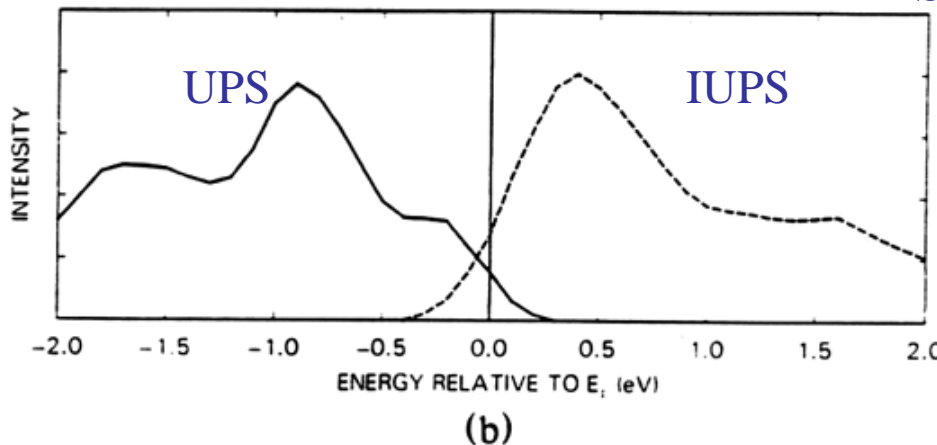
Shell model

$$N = 1 + \sum (10p^2 + 2)$$

STS of Si(111)-(7x7)



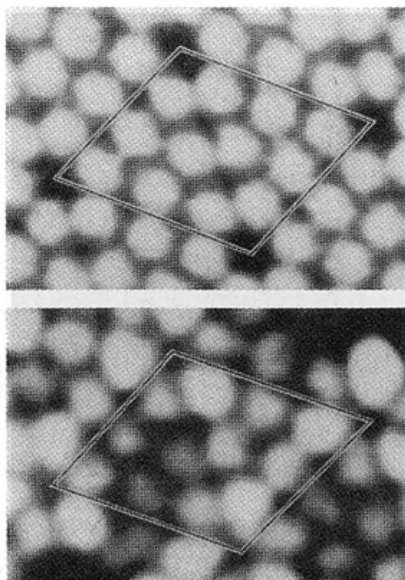
Science 234, 304 (1986).



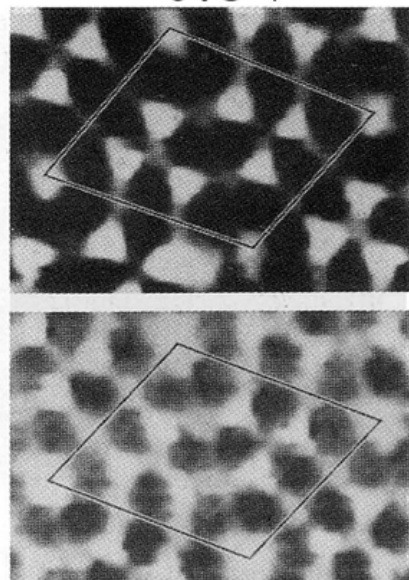
STS of Si(111)-(7x7)

topograph

+2V

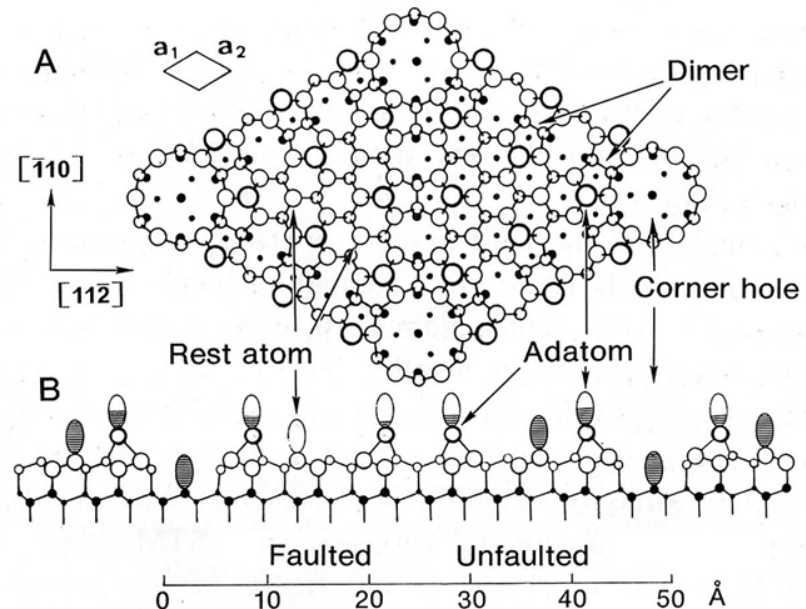


-0.8V



-0.35V

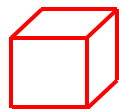
-1.8V



1. Science 234, 304-309 (1986).
2. Phys. Rev. Lett. 56, 1972-1975 (1986).

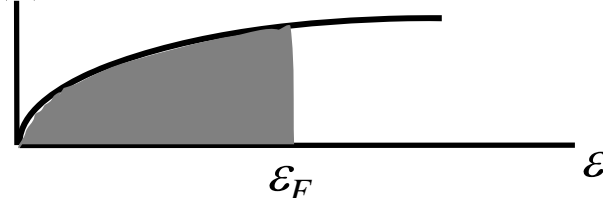
Density of states of various dimensions

3D



$$D(\varepsilon) \sim \varepsilon^{1/2}$$

$D(\varepsilon)$

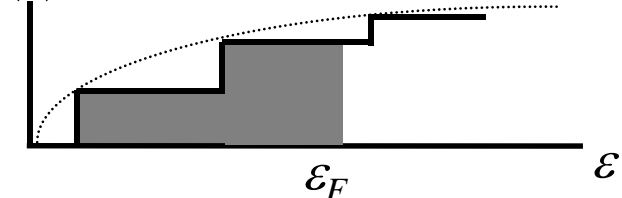


2D



$$D(\varepsilon) = m^* / \pi \hbar^2$$

$D(\varepsilon)$

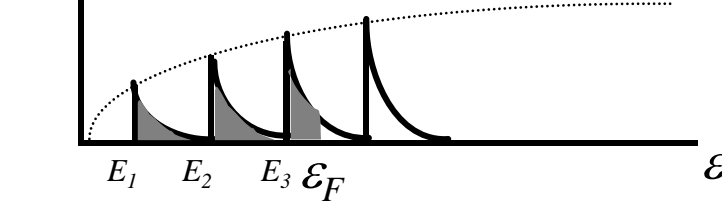


1D



$$D(\varepsilon) \sim (\varepsilon - E_n)^{-1/2}$$

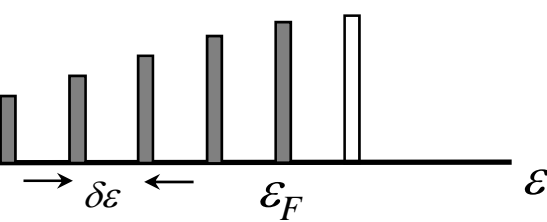
$D(\varepsilon)$



0D



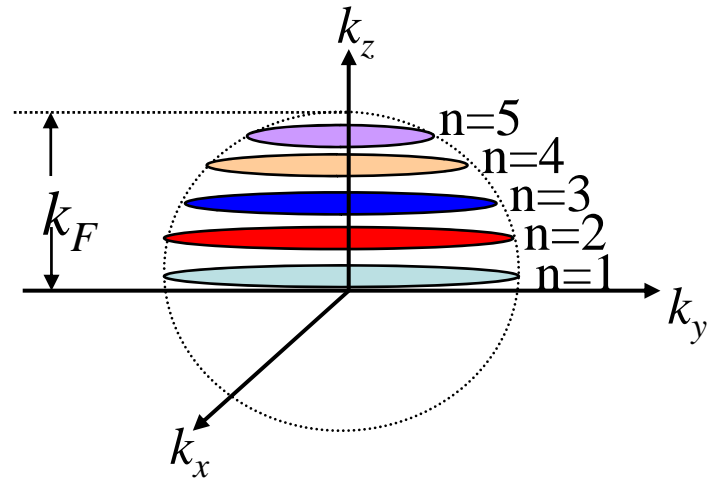
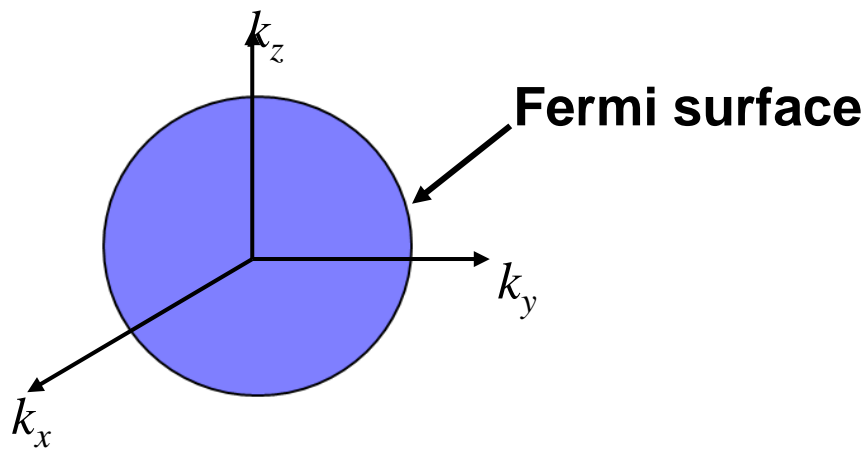
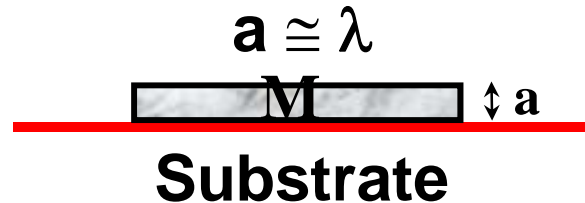
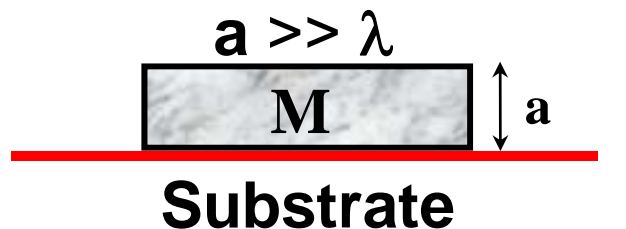
$D(\varepsilon)$



Quantum size effect

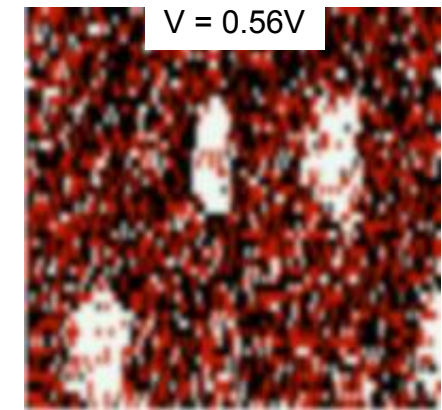
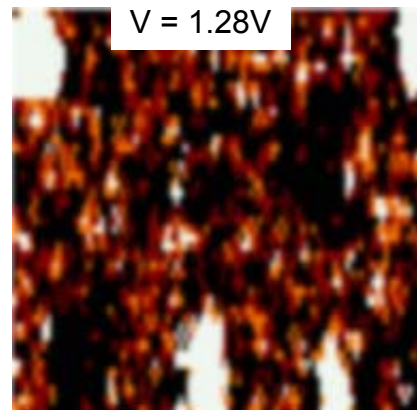
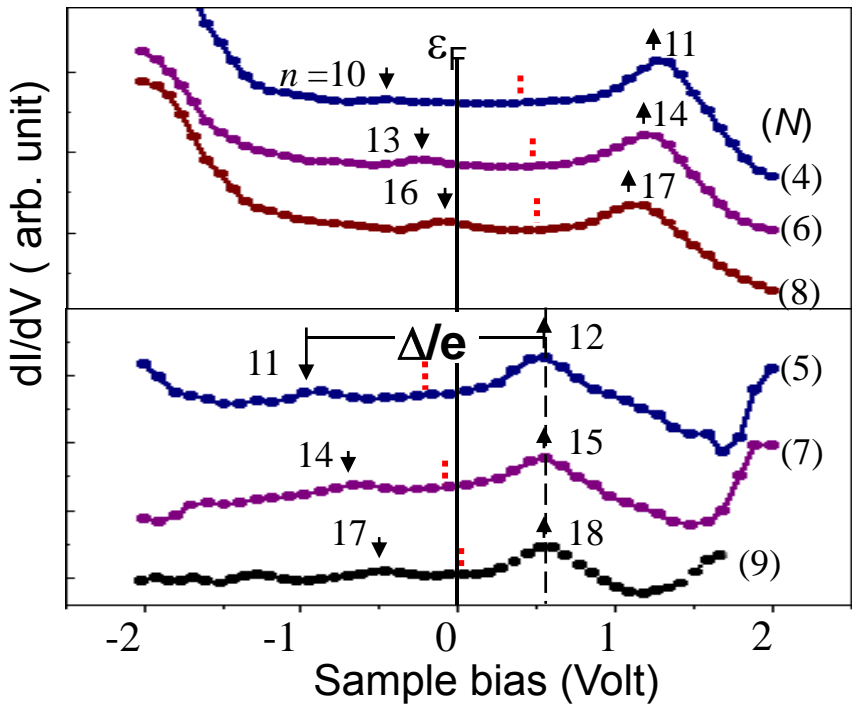
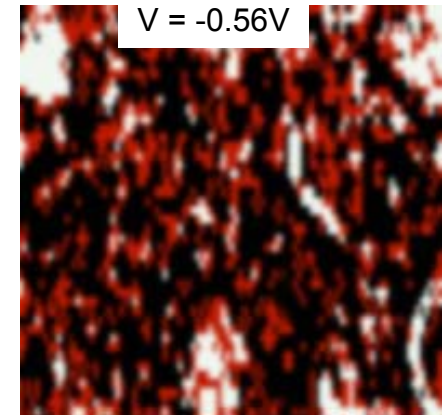
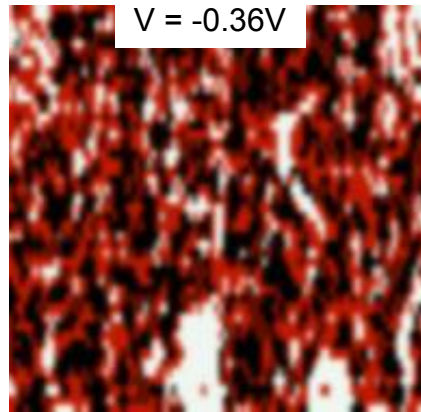
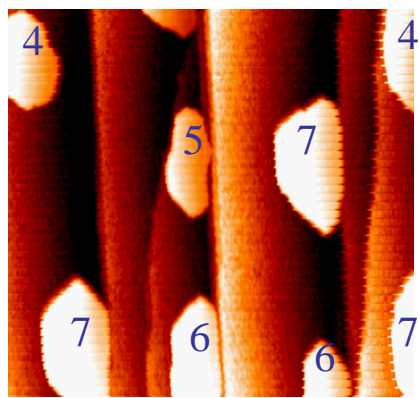
λ = de Broglie wavelength of electron

a = thickness of metal film



Spectroscopic images

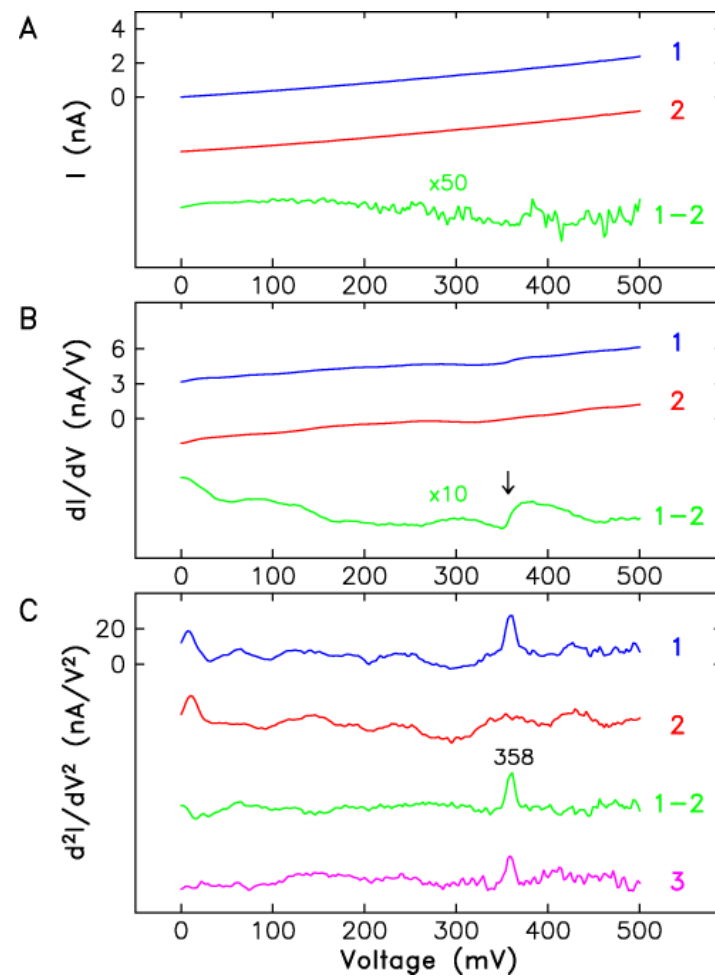
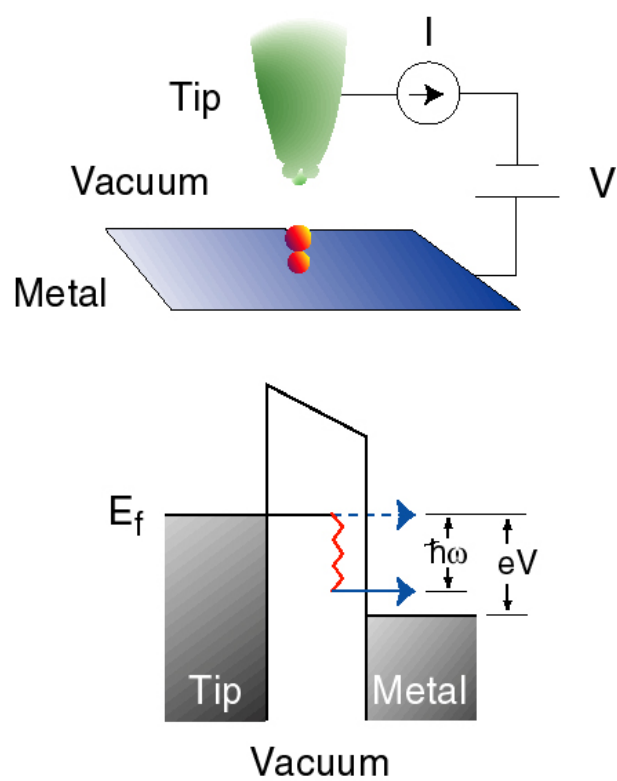
Topography



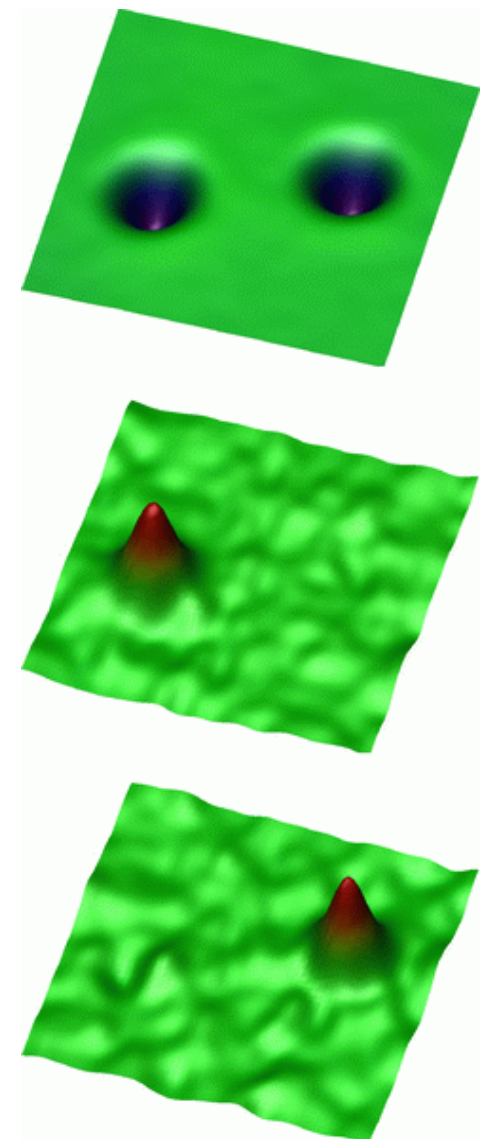
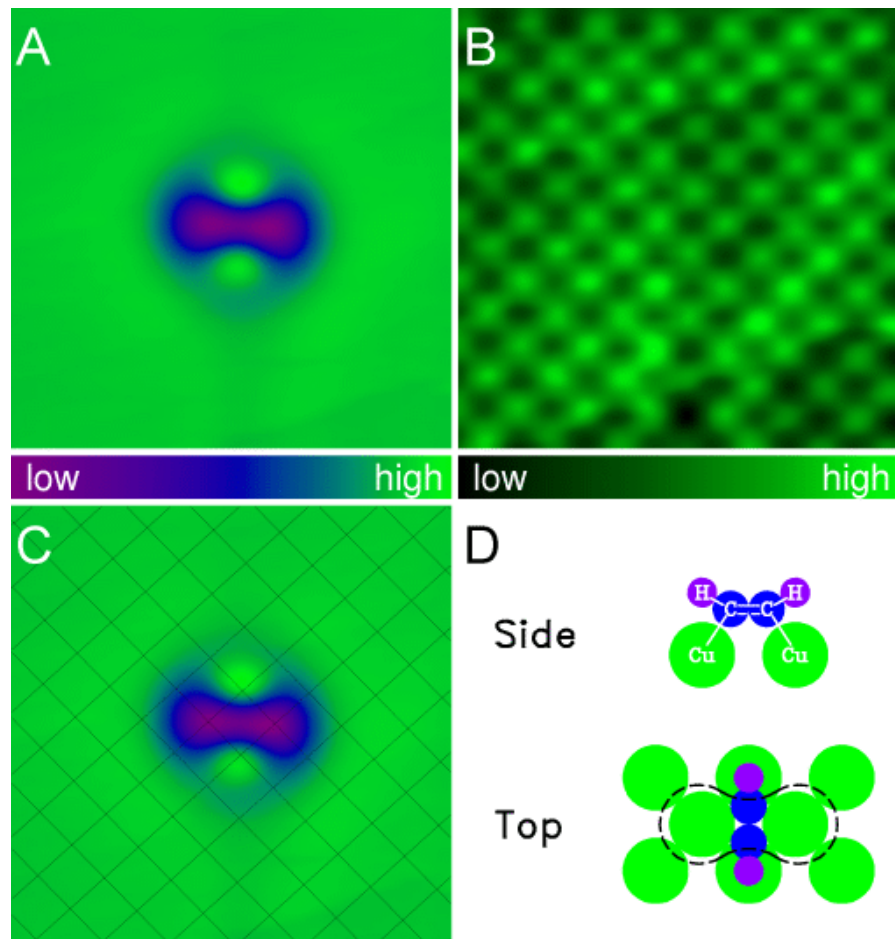
dI/dV mapping

Inelastic Tunneling

Elastic vs. Inelastic Tunneling

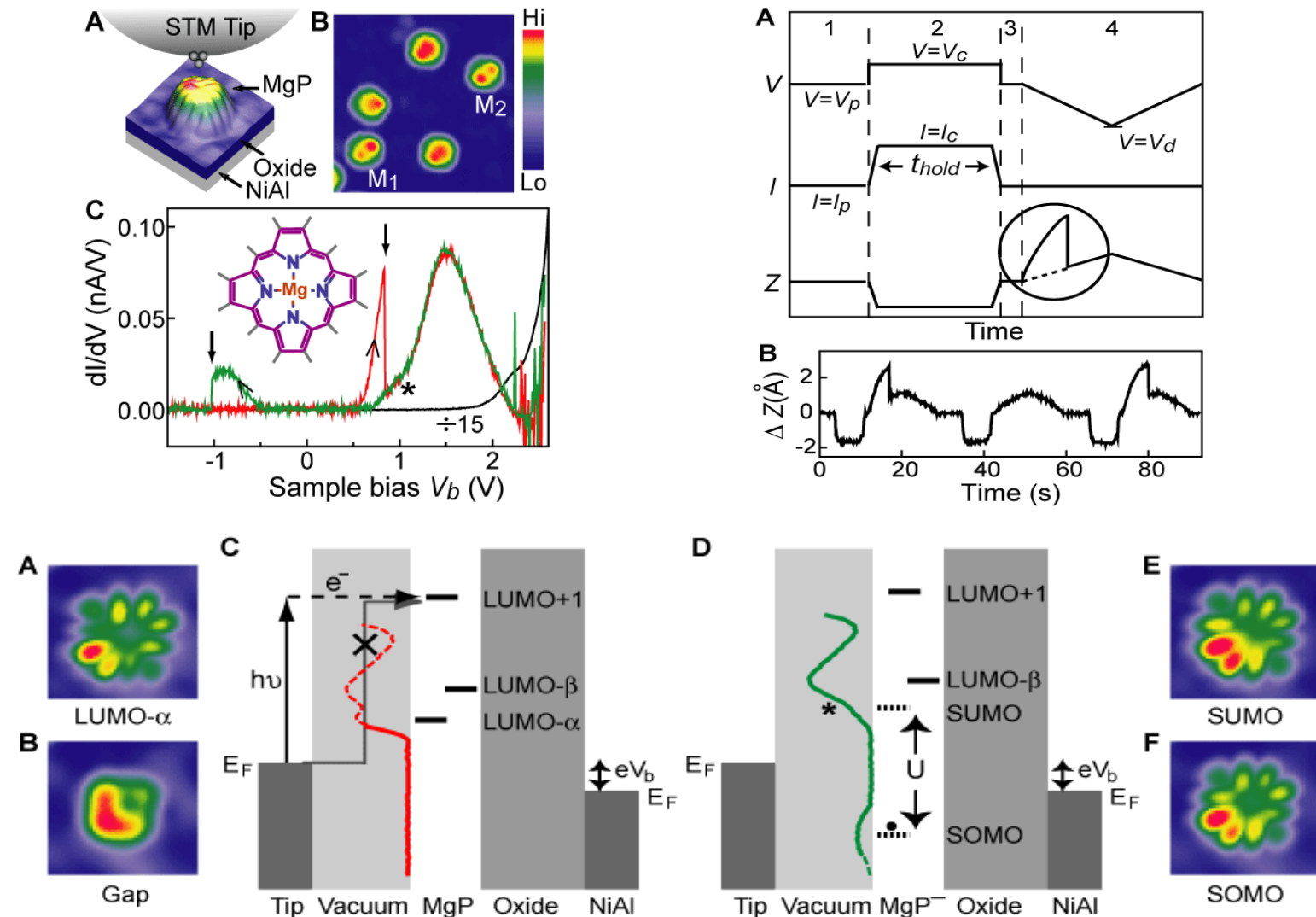


Single Molecule Vibrational Spectroscopy and Microscopy



B.C. Stipe, M.A. Rezaei, and W. Ho,
Science **280**, 1732-1735 (1998).

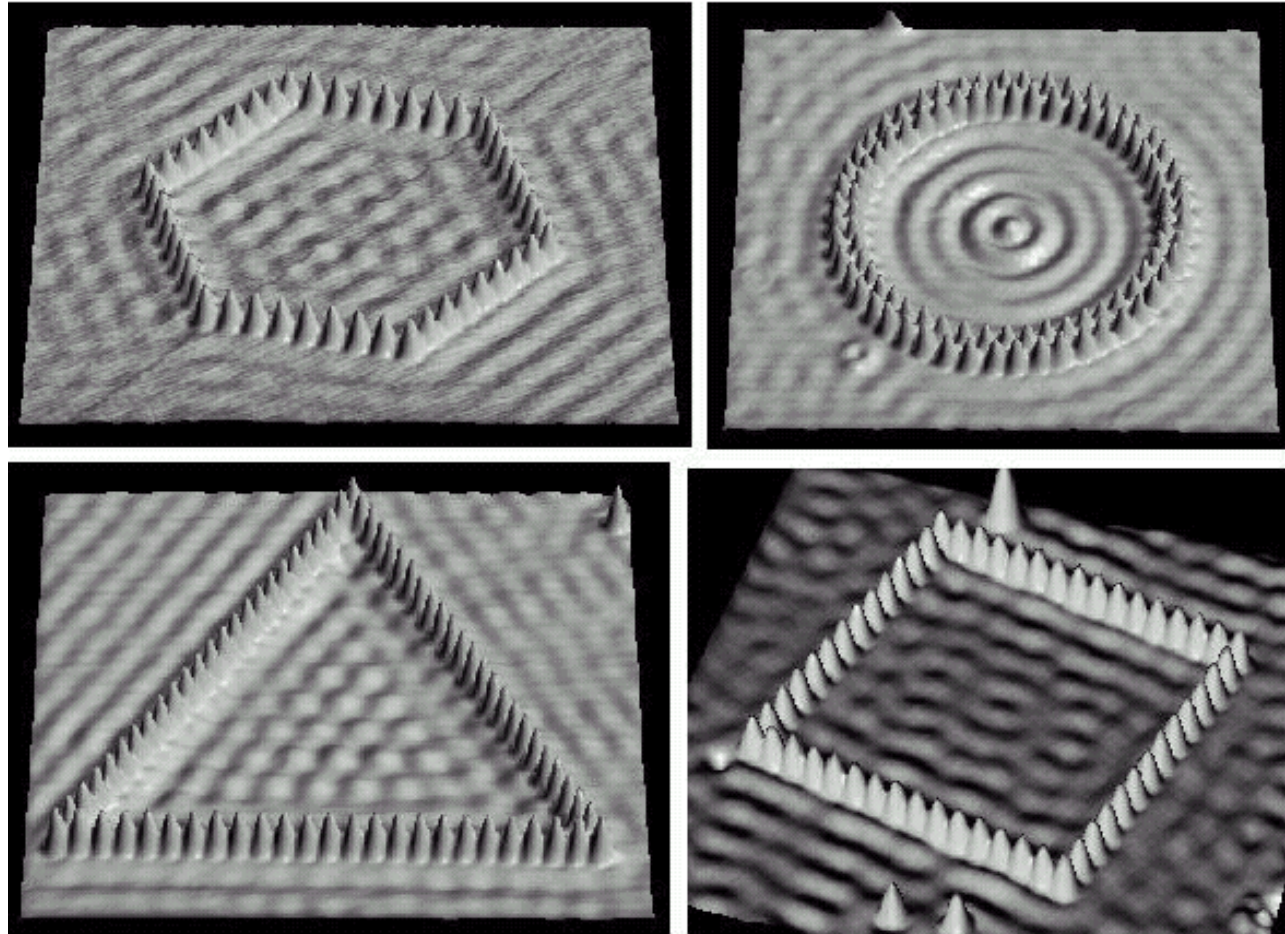
Atomic Scale Coupling of Photons to Single-Molecule Junctions



S.W. Wu and N. Ogawa and W. Ho, Science 312, 1362-1365 (2006)



Quantum corral



D.M. Eigler, IBM, Amaden

Artificial atom

